Three years of the Lightning Imaging Sensor onboard the International Space Station: Expanded Global Coverage and Enhanced Applications

Richard J. Blakeslee[1], Timothy J. Lang[1*], William J. Koshak[1], Dennis Buechler[2], Patrick Gatlin[1], Douglas M. Mach[3], Geoffrey T. Stano[2], Katrina S. Virts[2], Thomas Daniel Walker[2], Daniel J. Cecil[1], Will Ellett[2], Steven J. Goodman[4], Sherry Harrison[2], Donald L. Hawkins[2], Matthias Heumesser[5], Hong Lin[2], Manil Maskey[1], Christopher J. Schultz[1], Michael Stewart[2], Monte Bateman[3], Olivier Chanrion[5], and Hugh Christian[2]

[1]*NASA Marshall Space Flight Center, Huntsville, Alabama*

[2]*University of Alabama in Huntsville, Huntsville, Alabama*

[3]*Universities Space Research Association, Huntsville, Alabama*

[4]*Thunderbolt Global Analytics, Owens Cross Roads, Alabama*

[5]*Technical University of Denmark, Kongens Lyngby, Denmark*

Submitted to *Journal of Geophysical Research: Atmospheres*

Revised 10 June 2020

*Corresponding Author Address
Timothy J. Lang
NASA Marshall Space Flight Center (ST11)
Huntsville, AL 35812
(256) 961-7861, timothy.j.lang@nasa.gov

Abstract

The Lightning Imaging Sensor (LIS) was launched to the International Space Station (ISS) in February 2017, detecting optical signatures of lightning with storm-scale horizontal resolution during both day and night. ISS LIS data are available beginning 1 March 2017. Millisecond timing allows detailed intercalibration and validation with other spaceborne and ground-based lightning sensors. Initial comparisons with those other sensors suggest flash detection efficiency around 60% (diurnal variability of 51-75%), false alarm rate under 5%, timing accuracy better than 2 ms, and horizontal location accuracy around 3 km. The spatially uniform flash detection capability of ISS LIS from low-Earth orbit allows assessment of spatially varying flash detection efficiency for other sensors and networks, particularly the Geostationary Lightning Mappers. ISS LIS provides research data suitable for investigations of lightning physics, climatology, thunderstorm processes, and atmospheric composition, as well as realtime lightning data for operational forecasting and aviation weather interests. ISS LIS enables enrichment and extension of the long-term global climatology of lightning from space, and is the only recent platform that extends the global record to higher latitudes (± 55°). The global spatial distribution of lightning from ISS LIS is broadly similar to previous datasets, with globally averaged seasonal/annual flash rates about 5-10% lower. This difference is likely due to reduced flash detection efficiency that will be mitigated in future ISS LIS data processing, as well as the shorter ISS LIS period of record. The expected land/ocean contrast in the diurnal variability of global lightning is also observed.

Plain Language Summary

The Lightning Imaging Sensor on the International Space Station (ISS LIS) has been operating on-orbit since February 2017. The instrument has met all of its major science objectives, including detecting lightning day and night, identifying the specific locations within storms that are producing lightning, millisecond timing accuracy, and high probability of detecting lightning. The instrument also measures energy emitted by lightning, provides background images of storms and their surroundings, and delivers realtime lightning data. This has enabled enrichment and extension of the long-term global climatology of lightning from space, and provides more recent extension of the global record to higher latitudes (+/- 55 degrees). In addition, the instrument is serving as a standard for comparison to other spaceborne lightning sensors, such as the Geostationary Lightning Mapper (GLM). The realtime data from ISS LIS have enabled new applications for the benefit of the public, including weather forecasting and public safety. Finally, ISS LIS - in conjunction with other satellite instruments - is providing opportunities for new scientific study in areas such as lightning physics, thunderstorm processes, and atmospheric composition.

Key Points

1. The Lightning Imaging Sensor (LIS) has been providing data from the International Space Station (ISS) since March 2017.
2. ISS LIS provides storm-scale resolution (4-km) and millisecond timing of global lightning with spatially uniform detection efficiency (~60%).
3. The 3-year global lightning climatology is consistent with previous studies (within 5-10%), while extending results to higher latitudes.

1. Introduction

Lightning is a spectacular and direct response to strong thundercloud electric fields, which in turn are generated by intense atmospheric moist convection and (normally) the onset of active precipitation processes involving ice particles [*Saunders*, 2008]. Since lightning is inherently coupled to storm microphysics and dynamics, it can be used as a valuable tool to help remotely probe the developmental state, severity, and evolution of thunderstorms and thunderstorm complexes [e.g., *Yoshida et al.*, 2017; *Darden et al.*, 2009 and references therein]. Because a lightning discharge produces lightning nitrogen oxides (LNO_x), which in turn affect greenhouse gas concentrations (such as ozone), lightning also serves as a key indicator for monitoring long-term climate change [*Williams*, 2020], and plays an important role in affecting air quality forecasts [*Koshak et al.*, 2014a,b; *Koshak et al.*, 2015]. Overall, lightning provides useful information about a variety of atmospheric processes and offers vital scientific insight across a broad range of disciplines, such as weather, climate, atmospheric chemistry, and lightning physics. In addition, lightning itself is a direct threat to public safety, and also frequently impacts equipment and infrastructure on the ground.

The Lightning Imaging Sensor (LIS) on the International Space Station (ISS) plays a special role in improving our understanding of these complex interrelationships by providing global measurements of total lightning at high spatial and temporal resolution. This optically based lightning detection instrument was launched to the ISS in February of 2017, and has successfully operated with limited downtime since then. The ISS, which is in a low-Earth orbit (LEO) inclined near 55°, has been increasingly used as a host for a number of Earth-observing instruments due to its accessibility; ample space, power, and data bandwidth; and ability to precess through the diurnal cycle.

This paper will describe the ISS LIS instrument and its data products, document key performance metrics and science results from its first three years on orbit, discuss applications enabled by near-realtime ISS LIS data, and point toward new opportunities for cross-platform science that are enabled by using ISS LIS in conjunction with other Earth-observing instruments.

2. ISS LIS instrument and data structure

The ISS LIS measurement concept is based on time-differenced geolocated images at 777.4-nm wavelength [*Christian et al.*, 1989], an oxygen-absorption line that enables detection of lightning signals at cloud top during both day and night. The instrument consists of narrowband-filtered optics coupled to a 128 x 128 pixel focal plane. At the ~400-km altitude of the ISS, this provides nadir pixel resolution of ~4 km. The data processing follows Mach et al. [2007]. The first component of the data structure is events, which correspond to individual pixels that exceed the background level by a given threshold during a particular frame (2 ms). Adjacent events are clustered into groups when they occur within the same frame. Groups are then clustered into flashes when they occur close in time and space to one another. ISS LIS also provides quantitative information about optical energy output from lightning.

The ISS LIS instrument heritage spans multiple decades. The National Aeronautics and Space Administration (NASA) Marshall Space Flight Center (MSFC) - along with support from other science, academic, and commercial partners - developed a unique space-based lightning detection instrument, the Optical Transient Detector (OTD). The instrument design concept began in earnest in the 1980s with high-altitude aircraft measurements of lightning optical signatures at cloud top [*Christian et al., 1983*]. These measurements helped determine optimal space-based instrument requirements (e.g., what sensitivity would be required to detect lightning under both day and night conditions). The OTD was then engineered from these requirements in the early 1990s, and was launched aboard the MicroLab-1 satellite in 1995 from Vandenberg Air Force Base. It provided the first global-scale lightning climatology for its operational lifetime (1995-2000) [*Christian et al.*, 2003].

The OTD was essentially a prototype design for the LIS concept developed as part of the NASA Earth Observing System (EOS). The LIS was selected as an EOS instrument to fly on both a polar platform and the ISS, then known as Space Station Freedom. However, LIS instead was moved to the Tropical Rainfall Measuring Mission (TRMM) instrument complement because it had strong synergies with the core TRMM science instruments [*Kummerow et al.*, 1998]. TRMM LIS was launched in November of 1997 and ended its mission with the deorbiting of the TRMM satellite in April of 2015, a very successful 17+ years of operational lifetime.

Building on this long and dynamic heritage, the flight spare instrument for TRMM LIS was adapted to work on the ISS platform, resulting in ISS LIS. ISS LIS was part of the 5th Space Test Program - Houston mission (STP-H5), which is sponsored by the US Department of Defense (DoD). ISS LIS is currently located on the Express Logistics Carrier 1 (ELC-1) module of the ISS (Fig. 1). Given TRMM LIS's long operating period, ISS LIS is expected to be capable of operating for many years into the future. However, this is subject to the NASA senior review process for long-term missions.

Relative to TRMM LIS, ISS LIS extends the program of record for global coverage of low-latitude lightning (± 38°). Relative to OTD (which was in a 70° inclined orbit), ISS LIS extends the program of record for higher latitude lightning (up to ± 55°). And relative to geostationary lightning sensors, ISS LIS enables fully global-scale coverage as well as cross-platform validation. ISS LIS also has better spatial resolution (4 km) than either OTD or current geostationary sensors. Thus, ISS LIS is a unique and complementary Earth-observing instrument that provides near-realtime observations of lightning, including global-scale coverage to high latitudes (observing areas that produce an estimated 98% of all global lightning) throughout the diurnal and seasonal cycles.

In terms of NASA EOS Data and Information System (EOSDIS) Data Processing Levels, the ISS LIS science data are Level 2 (i.e., derived geophysical variable), while the background data are Level 1B (i.e., reconstructed instrument data processed to sensor units). The data are available in the TRMM LIS heritage Hierarchical Data Format Version 4 (HDF4) as well as the modern Network Common Data Format Version 4 (netCDF4), with corresponding browse images in Graphics Interchange Format (GIF).

ISS LIS products are generated and distributed by the NASA Global Hydrology Resource Center (GHRC) Distributed Active Archive Center (DAAC; Figs. 1 and 2) and can be discovered via the NASA Earthdata Search tool [*Earthdata*, 2020], the GHRC Hydrology Data Search Tool [*HyDRO*, 2020], and the GHRC website for ISS LIS [*ISS LIS*, 2020].

The LIS measurement concept was recently adapted to work from geostationary orbit [*Goodman et al.*, 2013; *Rudlosky et al.*, 2018]. This enables operational applications using continuous spaceborne lightning observations over a hemispheric field of view (FOV) [*Bruning et al.*, 2019].

3. Analysis and Findings

ISS LIS has operated successfully for more than three years. Among many other accomplishments, all major science objectives for the instrument have been achieved. In addition, a climatology of global lightning has been produced and compared to similar datasets. Cross-platform validation against other datasets has been performed, and new cross-platform science applications are being developed. Finally, a diverse user community is developing due to applications enabled by near-realtime ISS LIS data. These results are summarized in the subsections below.

3.1 Achievement of major science objectives

A primary and fundamental accomplishment in the past 3 years has been the successful achievement of all major science objectives of the instrument. These objectives include the detection of lightning during day and night, with storm-scale spatial resolution, millisecond timing, and high flash detection efficiency without a land/ocean bias. ISS LIS was designed to measure radiant energy and provide background images/intensity, and its deployment on the ISS enables the delivery of realtime lightning data. These objectives were achieved by successfully meeting several instrument/platform requirements. Most of these are discussed in Appendix A. Below we focus on validation of timing and geolocation accuracy, detection efficiency, and false alarm rate. Note that, as detailed in Appendix A, we expect an improvement of 2-5% in many of the instrument performance parameters discussed below based on planned future improvements to ISS LIS data processing.

Like TRMM LIS, ISS LIS has a frame rate of 500 s^{-1}. This implies a native 2-ms timing precision. The actual on-orbit timing *accuracy* of ISS LIS was determined by comparison against multiple ground-based and spaceborne reference datasets. The ground-based reference datasets were the EarthNetworks Global Lightning Network (ENGLN) [e.g., *Marchand et al.*, 2019], which operates wideband sensors (1 Hz to 12 MHz), and the Vaisala Global Lightning Dataset 360 (GLD360) [e.g., *Rudlosky et al.*, 2017], which detects waveforms in the very low frequency range (VLF; ~500 Hz to ~50 kHz). Both of these are global datasets. The spaceborne reference datasets were the Geostationary Operational Environmental Satellite (GOES) 16 and 17 Geostationary Lightning Mappers (GLM-16 and GLM-17) [*Goodman et al.*, 2013, *Rudlosky et al.*, 2018]. GLM is built on the LIS/OTD optical detection heritage and is sensitive to both intracloud (IC) and cloud-to-ground (CG) lightning.

The timing data as initially received from ISS exhibited offsets up to ± 1 s with respect to the reference data, with an alternating drift pattern that cycled approximately every 9 days. This drift was accurately characterized based on careful analysis. On the basis of this, timing correction variables, and an additional constant offset, were applied to produce the current timing accuracy (Fig. 3 left).

After correction, ISS LIS has modal temporal offset of +1 ms, or approximately one-half the LIS frame duration, when compared with GLM-16/17 (Fig. 3 left). The standard deviation in the offset is less than 2 ms in either direction, compared to GLM-16/17. This comparison was based on group timings between ISS LIS and the GLM datasets. Relative to the ground-based reference datasets, there is zero modal offset, and the standard deviation is also below 2 ms. Thus, after correction for the ISS timing errors, the ISS LIS timing accuracy is less than the native timing precision of the instrument itself (2 ms). This is similar to the independent analysis performed by *Erdmann et al*. [2020], using a different reference dataset, and is consistent with (though not as precise as) the timing analysis for TRMM LIS by *Bitzer and Christian* [2015].

ISS LIS geolocation accuracy was analyzed through a coordinate system transform technique that allowed LIS location errors with respect to the reference data to be displayed in the native LIS field-of-view. This analysis revealed that the ISS navigation variables used for LIS geolocation vary systematically during each orbit, creating location errors of up to 25 km. This particular issue was unrelated to the TRMM LIS geolocation issue discussed by *Zhang et al*. [2019]. The ISS LIS team worked diligently to troubleshoot the initial issues with geolocation (and timing), as these posed complex interconnected problems that required focused analysis and skilled interpretations to resolve.

An iterative tuning process resolved these initial problems and produced corrected geolocation data and the current analysis of ISS LIS spatial accuracy (Fig. 3 right). Relative to GLM-16/17, corrected ISS LIS spatial offsets are almost entirely less than 10 km, with the vast majority below 5 km. Offsets relative to ENGLN and GLD360 are distributed more broadly, but for each of the spaceborne and ground-based reference datasets the modal offset is approximately 2-3 km. This means that ISS LIS has achieved sub-pixel (< 4 km) location accuracy. The independent analysis by *Erdmann et al*. [2020] supports this assessment.

Timing, location, flash DE, and false alarm rate (FAR) have been stable during most of the mission to date. Figure 4 shows the time series of these parameters through early 2020. ISS

LIS temporal accuracy offset shifted by about 1 ms on 16 December 2018, such that LIS now slightly leads the reference data (Fig. 4 top). A few larger deviations occurred during two periods in early 2019, related to atypical ISS maneuvers. However, in most circumstances the absolute magnitude of the offsets remain less than 2 ms. LIS geolocation accuracy also has been stable throughout the mission (Fig. 4 middle), with the modal peak of the offset normally less than 5 km. The detection performance of ISS LIS is also stable over time (Fig. 4 bottom), aside from the known deviations in early 2019 mentioned above. The flash DE (calculated using a 50-km, 200-ms matching window) is stable with respect to each of the reference datasets (64% relative to GLM, and 56-57% relative to ENGLN/GLD360), and the FAR, calculated over the Americas domain where the greatest quantity and best quality reference data are available, is under 5% on average. This is a higher FAR than that published for TRMM LIS [*Boccippio et al.*, 2002], but that study did not include the impact of specular reflections (e.g., cloud and ocean glint) like this analysis did. The flash DE is comparable to the values computed independently for ISS LIS by *Erdmann et al.* [2020].

Detection efficiency was also examined as a function of time of day (Fig. 5). As expected for optical instruments like ISS LIS, flash DE is maximized during local nighttime (64-75% near local midnight, depending on reference dataset) and minimized during local daytime (51-65% around 1700 LT, just before sunset/dusk). There is another apparent minimum in flash DE against GLM-16, around sunrise (~0600 LT); however, the analysis includes a period of time before the GLM-16 blooming filter was implemented to reduce the impact of solar glint. Since a similar sunrise decrease is not observed in the glint-filtered GLM-17 data, we infer that this reduction in DE against GLM-16 is primarily caused by increased GLM-16 false alarms during local sunrise.

Analysis of TRMM LIS DE versus the ground-based reference datasets indicates that ISS LIS DE is approximately 4-7% lower overall compared to TRMM LIS (using 2014-2015 ENGLN and GLD360 data; not shown). As mentioned previously (and explained in Appendix A), we expect increases of ~2-5% in flash DE after planned ISS LIS dataset processing improvements. In addition, the ground networks often improve each year [e.g., *Rudlosky et al.*, 2017], and this may also explain some of the DE discrepancy between the ISS LIS and TRMM LIS eras (i.e., the ground networks are likely detecting more lightning now versus 5+ years ago). Finally, there is a possibility that ISS LIS is slightly less sensitive than TRMM LIS. Future work will attempt to quantify any LIS instrument sensitivity differences, if they exist.

Note that none of the above flash comparisons follows the Bayesian approach of *Bitzer et al.* [2016]. That study found a similarly low TRMM LIS detection efficiency against ground networks (~53%), but when corrected within a Bayesian probability framework the estimated detection efficiency increased to 80%. Bayesian analysis of ISS LIS detection efficiency is planned in the future.

3.2 Lightning climatology

The ISS LIS lightning climatology has been completed for the first three years of data (March 2017 - Feb 2020; Fig. 6a). Within ± 38° latitude, these results are broadly similar to the more than 13-year (after orbit boost; September 2001 - December 2014) TRMM LIS climatology (Fig. 6b). During this period, TRMM had a nominal orbit altitude of 402.5 km - very similar to the ISS orbit altitude range of 400-405 km. (The TRMM pre-boost orbit altitude was substantially lower, at 350 km, and thus is not considered here to keep the comparison more direct.)

Because ISS LIS has a shorter period of record (3 years vs 13 years), the lightning density maps are not as smooth despite the 0.5° gridding (Fig. 6a). There are also sampling limitations over low flash rate regions, such as the global oceans. However, notable hotspots [*Albrecht et al.*, 2016] from the TRMM LIS climatology (Fig. 6b), such as central Africa, Paraguay/northern Argentina/Rio Grande do Sul (Brazil), Lake Maracaibo (Venezuela), the Himalayas/Indian Subcontinent, and the Maritime Continent stand out, and feature comparable flash rate densities between ISS and TRMM LIS. For example, peak flash rate densities over central Africa exceed 80 km^{-2} yr^{-1} in both datasets. The well-known stark contrast between land and ocean lightning flash rate densities also stands out in both plots, as do the coastal enhancements in lightning over the Gulf Stream, near west Africa, the Caribbean and near Central America, near southeastern Brazil, the Bay of Bengal, etc. Despite the more limited sampling, ISS LIS also has been able to observe the small enhancements in lightning over the open Pacific, between ± 30° latitude, west of -120° (south Pacific) and -150° (north Pacific) longitude (including the Intertropical Convergence Zone, ITCZ). This is similar to TRMM LIS (Fig. 6b), but the patterns are more diffuse due to fewer samples. Note that portions of this more active ocean region are now under continuous observation by GLM-17. Additional notable lightning features that weren't fully observed by TRMM LIS include enhancement over the Tien Shan mountain range near northwest China, and a slight enhancement over New Zealand (especially the north island).

In the global aggregate, lightning flash rates (between ± 38° latitude) are comparable between ISS LIS and TRMM LIS (Fig. 7). Both datasets show globally averaged flash rate ranging between 25 and 55 s^{-1}. In addition to significant annual and interannual variability, both datasets also appear to show semiannual variability in the global flash rate, which is consistent with *Williams* [1994]. This, along with Fig. 6, demonstrates that ISS LIS is making fundamentally similar observations to TRMM LIS, and thus is capable of extending the TRMM LIS dataset over the tropics and subtropics for a longer time period.

ISS LIS enables coverage of higher latitudes (± 55°) compared to TRMM LIS (± 38°), providing renewed viewing of regions not observed by spaceborne global lightning sensors since the OTD mission ended in 2000. For example, ISS LIS reenables more complete viewing of the Great Plains of the United States (US), which features flash rate densities ~30 km^{-2} yr^{-1} extending as far north as the border with Canada (Fig. 6a). The improved coverage of the continental US is a particularly important advantage of ISS LIS, because this coverage allows for a more robust examination of lightning/climate relationships within ongoing National Climate Assessment (NCA) studies [*Koshak*, 2017]. Another mid-latitude hot spot over Manchuria is also observed by ISS LIS, and the coastal enhancement of lightning near eastern South America is seen to extend further south. ISS LIS also provides coverage of most of Europe, including the lightning enhancement near the Alps. Lightning enhancement over Turkey is observed by ISS LIS.

The combined TRMM LIS and OTD dataset [*Cecil et al.*, 2014] provides a useful point of comparison for ISS LIS. OTD was in LEO orbit at 70° inclination and 740-km altitude [*Christian et al.*, 2003], so it provided coverage at higher latitudes than ISS LIS, but with reduced spatial resolution and geolocation accuracy. Table 1 shows a comparison of globally averaged flash rates from ISS LIS relative to the OTD and TRMM LIS climatology published by *Cecil et al.* [2014]. ISS LIS is measuring slightly lower flash rates, but the numbers are generally within 5-10% of the previous climatology, which is well within the magnitude of expected offset from the reduced effective detection efficiency in version 1 ISS LIS data (Section 3.1), the sampling limitations of the 3-year ISS LIS record, as well as interannual variability (e.g., Fig. 7). Even the relatively larger discrepancies seen between TRMM LIS/OTD and ISS LIS during December-February are reasonably attributed to the above causes as well, since the differences are still within ~15%. Note also that the ISS LIS global flash rates in Table 1 are not smoothed, unlike the TRMM LIS/OTD values.

Relative to *Cecil et al.* [2014], ISS LIS has observed potentially higher flash rate densities in notable mid-latitude areas - such as Turkey and the Middle East, southern Canada, Manchuria, Europe and Northern Africa (Fig. 6a). However, caution in interpreting the 3-year ISS LIS dataset is required, since the relative impacts of individual storms may be influencing these differences. Integration of ISS LIS observations into the full LIS/OTD gridded dataset, which will enable detailed quantitative comparisons for individual regions, is planned for a future study. This planned analysis should be able to determine if, and to what extent, lightning has increased globally at higher latitudes as a result of climate change, relative to the OTD era (1995-2000) [e.g., *Veraverbeke et al.*, 2017; *Williams*, 2020].

The seasonal distribution of lightning from ISS LIS also follows expectations established by previous global climatologies (Fig. 8). Globally, lightning is maximized during June-August (Fig. 8b); however, both March-May and September-November also have significant activity

(Fig. 8a, c). Notably, in boreal autumn the northern Great Plains of the US can remain active, even as similar latitude locations in Europe, for example, see a substantial decrease from the summertime peak (Fig. 8c). The Manchuria lightning peak is primarily a boreal summertime phenomenon, with a significant decrease in both spring and fall. Lightning in the Middle East is most prevalent during boreal spring and fall, providing evidence for a semiannual signal in lightning in certain regions of the globe [*Williams*, 1994]. Turkey reaches its maximum in summer. Boreal winter leads to a significant reduction in northern hemisphere lightning (Fig. 8d); however, there are noticeable hot spots remaining in the US Gulf Coast. The lightning peak near Paraguay is most distinctive during austral spring (Fig. 8c). These basic seasonal patterns are also observed in the TRMM LIS/OTD dataset [*Cecil et al.*, 2014].

Globally averaged diurnal variability of lightning (Fig. 9) follows the typical patterns observed in previous climatologies [*Virts et al.*, 2013; *Blakeslee et al.*, 2014; *Cecil et al.*, 2014]. Namely, the diurnal cycle over land drives the overall global diurnal variability in lightning, with the ocean flash rate essentially flat throughout the day and night. On average, lightning peaks in the local afternoon (3-4 pm Local Solar Time, LST), and reaches a minimum near 10 am LST (Fig. 9a). The timing and the approximate dynamic range in the LST reference frame (15-100 s^{-1}) are comparable to the analysis of *Blakeslee et al*. [2014] for TRMM LIS/OTD. Viewed in UTC time coordinates (Fig. 9b), lightning follows the classic Carnegie-like curve structure [*Mach et al*., 2011], peaking during 18-19 UTC. The timing and the 30-60 s^{-1} dynamic range are very close to *Blakeslee et al*. [2014] as well. Note that the approximately 2x larger global diurnal variability in flash rate, versus the diurnal variability of electric field in the Carnegie curve, is explained by the effect of higher currents in oceanic thunderstorms, as well as the influence of electrified shower clouds [*Mach et al.*, 2009; 2010; 2011].

3.3 Use as a tool for GLM calibration and validation

A high-priority effort at NASA MSFC has been to properly validate the GLM instruments on GOES-16 and GOES-17. This includes examining the GLM flash detection efficiency (DE), the flash false alarm rate, the lightning location/timing accuracy, maximum data rate capability, and long-term instrument degradation. Specific GLM instrument requirements have to be validated to confirm that GLM performance is acceptable for critical operations and decision making. GLM validation often makes use of several different ground-based lightning detection networks. These are high-quality data sources, but they are all land-based. A large part of the GLM FOV, especially GLM-17, is over the ocean where the quality of ground-truth data is highly variable. Fortunately, ISS LIS has provided vital data of uniform quality out over the oceans.

Another problem with comparing GLM to ground sources is that the comparison is not truly one-to-one. The GLM is an optical sensor, whereas all of the ground-based networks consist of RF sensors. The RF sensors look at fundamentally different physics and different parts of the lightning flash, making one-to-one comparisons difficult. Since ISS LIS is an optical sensor very similar to GLM (though with approximately 4x better spatial resolution), it is the only source of direct comparison for GLM. Indeed, because ISS LIS is a heritage sensor of GLM, with similar operation and data structure, it has provided particularly easy/efficient inter-comparisons (i.e., both optical, both spaceborne, and both detect lightning over land/ocean).

GLM-16 has been observed to have a substantially depleted flash DE over the northwestern CONUS (e.g., Washington and surrounding states). A detailed plot of GLM-16 flash DE for the period January 2018 to December 2019 is shown in Fig. 10. The GLM flashes were compared with observations from ISS LIS (Fig. 10 left), as well as data derived from two ground-based RF lightning detection networks - ENGLN (Fig. 10 middle) and GLD360 (Fig. 10 right). All three comparison datasets agree on the basic structure of GLM-16's northwestern CONUS DE depletion (reduced to as low as 20-40%). The fact that both optical spaceborne (ISS LIS) and RF ground-based (ENGLN and GLD360) measurements agree provides increased confidence that the DE depletion is the result of GLM instrument effects near the edges of its FOV.

ISS LIS continues to provide important one-to-one comparisons with GLM data, and will remain a key dataset for current and future GLM validation [e.g., *Zhang and Cummins*, 2020], as well as potentially other future geostationary lightning observations, such as from the forthcoming Meteosat Third Generation (MTG) Lightning Imager (LI) [*Kokou et al.*, 2018]. ISS LIS further provides a single observation system that will enable direct intercomparisons between GLM, LI, and other space-based observations.

3.4 ISS LIS data products and user community

Unlike its predecessor, ISS LIS has the ability to transmit and disseminate lightning data in near real time. This ability is significant as it enables usage of ISS LIS in operational applications. The near-realtime capabilities are particularly beneficial in data-sparse regions, such as over oceans, to contribute to storm warnings, nowcasts, oceanic aviation, and international Significant Meteorological advisories (SIGMETs).

The near-realtime ISS LIS data are provided to the US National Weather Service (NWS) and other interested users in partnership with both NASA's Land, Atmosphere Near real-time Capability for EOS (LANCE) project and the Short-term Prediction Research and Transition (SPoRT) center [*Jedlovec*, 2013]. As ISS LIS detects total lightning (near globally) with high detection efficiency, it can therefore fill gaps in the depiction of lightning activity of interest to NWS forecasters over land and ocean areas. These data, as well as non-real-time analyses are being used by several applied and operational institutions to improve decision-making and to benefit humankind. These institutions include, for example, the NWS Pacific Region, the Aviation Weather Center (AWC), the National Hurricane Center (NHC), the Ocean Prediction Center (OPC), the World Weather Research Program (WWRP), and other government, business, and military organizations.

The GHRC DAAC coordinates with the LIS science team to process and archive ISS LIS datasets. The ISS LIS mission currently produces four products: (1) Near-realtime (NRT) science lightning data [*Blakeslee*, 2019a], (2) NRT background cloud scene data [*Blakeslee*, 2019b], (3) Non-quality-controlled (NQC) version 1 science lightning data [*Blakeslee*, 2019c], and (4) NQC background cloud scene data [*Blakeslee*, 2019d].

The NRT data are available within two minutes of observation and are appropriate for applications requiring low-latency data (e.g., AWC and NHC). NRT data and browse images age off the server after ten days and are not a static archived data collection. Due to the nature of NRT data transmission, some data may be missing. Hence, the NQC data are produced daily and are more complete than the NRT data. Although the version 1 NQC data have not been reviewed to assure data quality, they are more appropriate for science and applications with less stringent latency requirements. The version 1 NQC data have been validated, however, as described in Section 3.1, and are currently undergoing quality control that will be included in a future release.

These ISS LIS observations can be used to derive multiple products. Traditionally, the flash observation has been the most widely used, particularly in near real-time operations. This is a latitude/longitude point showing the centroid of the flash. This flash centroid is typically plotted as a density product (i.e., number of flash centroids per unit area).

The ISS LIS dataset has had widespread use in the past 3 years, with over 6,100 users to date. Specifically, the GHRC DAAC has tallied downloads of the data based on the end user's stated application (e.g., weather, climate, atmospheric composition, etc.). As with the OTD and TRMM LIS predecessors, there has always been an enthusiasm from the user community to apply lightning data in diverse ways, especially in weather and chemistry/climate studies. For the most recent full calendar year (2019), ISS LIS data made up two of the top five most downloaded datasets at GHRC DAAC. Two others, including the top dataset, were from the ISS LIS predecessor, TRMM LIS.

While not exhaustive, several uses of ISS LIS are described below, and demonstrate a variety of impacts by these observations. As mentioned previously, the NRT ISS LIS data are provided to the AWC. The AWC's area of responsibility covers vast oceanic regions. Just a single flash observation provides confirmation of a convective system to the AWC, enabling aircraft to be rerouted safely around these systems. Due to reduced DE during the day, as well as coarser pixel resolution off boresight, weaker and smaller size flashes are not as well detected by the GLM instruments [*Zhang and Cummins*, 2020]. For these reasons AWC and other NWS service centers have found that ISS LIS augments their confidence in GLM (and ground-based) detection of lightning especially over oceanic regions [*Goodman et al.*, 2020a]. AWC is able to display ISS LIS, GLM, and ground-based lightning data concurrently in a 10-min flash density grid overlay in their forecaster workstation displays. *Goodman et al.* [2020b] showed how the smaller pixel size, and more nadir view (relative to GLM), of ISS LIS can often detect lightning (and thus convective initiation) in developing storms sooner than other lightning datasets. Thus, while ISS LIS flash observations are vital to provide lightning observations in locations where ground networks and GLM are unavailable or have limited detection efficiency, they also are able to provide valuable information to forecasters even when other lightning observations are available.

The NRT data have also been an integral component of the World Meteorological Organization's (WMO) High Impact Weather Lake Systems (HIGHWAY) project [*Virts and Goodman*, 2020]. Centered on Lake Victoria in East Africa, the NRT ISS LIS data from NASA LANCE are used to monitor and provide quality assurance for ground-based total lightning data from the ENGLN to better characterize storms as observed by the European Organization for the Exploitation of Meteorological Satellites (EUMETSAT) Meteosat Second Generation (MSG) satellite. The goal of this effort is to better characterize, monitor, and predict thunderstorm development in this region to provide early warning to at-risk communities. This also serves as an operational demonstration to help prepare the community for MTG-LI.

Another collaborative project was with NASA DEVELOP (not an acronym) and GHRC DAAC. Here, data from both TRMM and ISS LIS were used to develop a lightning risk assessment for Bangladesh and Nepal [*Evans et al.*, 2018]. The LIS data provided the necessary lightning observations for the project. Instead of simply creating a lightning climatology, the DEVELOP team combined the lightning observations with socioeconomic information. The result (Fig. 11) gave the government authorities an easy-to-interpret view of where lightning was the greatest threat due to a combination of lightning activity, available shelter, and types of jobs. Such information can help government decision-makers direct funds to improve lightning safety in the most at-risk locations.

Lastly, the WMO has deemed lightning an Essential Climate Variable (ECV). Space-based observations play an integral role in providing global lightning coverage. The ISS LIS observations extend the record of the earlier OTD and TRMM LIS instruments, and are included with those instruments in the Global Climate Observing System (GCOS). As part of this, ISS LIS observations will be used as part of a proposed 10x10 km^2, global product that blends both space- and ground-based lightning observations into daily and monthly time scales [*Aich et al.*, 2018]. Additionally, these data extend the OTD and TRMM LIS period of record for use in understanding trends in global thunder days [*Lavigne et al*, 2019]. This supports continuing work to identify significant shifts in global lightning activity [e.g., *Williams*, 2020].

4. Current and future cross-platform science

Although ISS LIS observations have been used for assessments of current and future geostationary lightning mappers [*Erdmann et al.*, 2020; *Hui et al.*, 2020], they also offer very complementary information for other types of atmospheric investigations, described in the following subsections.

4.1. Investigations into the physical development of lightning discharges

Analyses of optical and combined optical/RF emissions from lightning have provided a wealth of insights on processes involved in the lightning discharge [*Suszcynsky et al.*, 2000; *Thomas et al.*, 2000; *Ushio et al.*, 2002; *Noble et al.*, 2004; *Østgaard et al.*, 2013; *Bitzer*, 2017; *Peterson et al.*, 2017; *Peterson and Rudlosky*, 2019; *Zhang and Cummins*, 2020]. Hence, the capability of ISS LIS to detect the optical fingerprint of lightning on a global scale with a relatively high detection efficiency makes for a unique dataset to compare with optical, RF, and other measurements of lightning and related atmospheric electrical phenomena.

Current and planned space-based missions to investigate lightning and upper atmospheric electrical phenomena include measurements across several parts of the electromagnetic spectrum that complement those obtained with ISS LIS. One of these is the Atmosphere-Space Interactions Monitor (ASIM), which is an instrument suite developed by the European Space Agency and installed on the ISS in April 2018 [*Neubert et al.*, 2019]. The imager onboard ASIM has a 42x slower frame rate than LIS, but it has a 10x greater pixel resolution at nadir than the LIS camera [*Chanrion et al*., 2019]. Furthermore, ASIM is capable of measuring light intensity across its FOV about 200x faster than LIS. This complementary nature of ASIM and LIS enables resolving the spatial and temporal components of lightning in more detail.

Both instruments detected a lightning flash on 7 February 2019, at 1941 UTC over Madagascar (Fig. 12). During its 150-ms duration, the flash illuminated three frames of the

ASIM camera, while LIS detected nine groups (i.e., collections of adjacent events in the same frame; c.f., Section 2). Figure 12 highlights one of these frames from the ASIM camera, along with the LIS events and temporal evolution of LIS groups and ASIM's 777.4-nm photometer. Each of the three LIS groups detected during this ASIM camera frame had a corresponding relative peak irradiance measured by the ASIM photometer. Although ASIM's photometer was able to detect these distinct flash subcomponents, LIS was used to locate where in ASIM's photometer FOV they occurred, which is especially important for separating multiple source regions within active thunderstorm complexes. One of the strokes illuminated 36 pixels of the LIS camera for 2 ms, and the higher-resolution ASIM camera observations revealed the narrowest part of the illumination at cloud top to be roughly half a LIS pixel wide (~2 km).

As shown above, when sub-pixel-sized lightning sources trigger ISS LIS detections, ASIM can be used to infer more information about the true spatial extent of that discharge. Also, curved channels within one or more pixels and dark regions between emitting parts of a cloud may not be resolved by LIS. Instead, the intensity measured by LIS would be proportional to the seemingly more active part of the cloud, obscuring whether the respective source was wider and less intense or small and bright [*Zhang and Cummins*, 2020].

Satellite missions such as ASIM and the upcoming Tool for Analysis of Radiation from lightning and Sprites (TARANIS) [*Lefeuvre et al.*, 2008], which focus on investigating transient luminous events (TLEs) and terrestrial gamma ray flashes (TGFs), will be compared with observations from ISS LIS for calibration and validation of their optical instruments and used to better determine the spectral fingerprint of these upper atmospheric electrical phenomena. Additionally, LIS observations are being compared with ground-based electric field measurements from Marx meter arrays in Panama [*Bitzer et al.*, 2013; *Zhu et al.*, 2020] to investigate signatures of TGFs measured at the ground to their optical characteristics observed in space. Marx meter arrays in Alabama, Panama, and Argentina also are being compared with ISS LIS to observations to further investigate the extent of optical emissions by narrow bipolar events [*Jacobson et al.*, 2013; *Rison et al.*, 2016; *Liu et al.*, 2018].

4.2. Precipitation and lightning in mid-latitude cyclones

Since ISS LIS operates during the era of the Global Precipitation Measurement (GPM) mission [*Hou et al.*, 2014; *Skofronick-Jackson et al.*, 2018], global observations of lightning and precipitation are being combined to expand upon related findings from TRMM in the tropics [*Petersen and Rutledge*, 2001; *Liu et al.*, 2012] and gain new insights of mid- and high-latitude storm systems. Coincident ISS LIS and GPM observations are being combined into a new lightning-enriched GPM-based Precipitation Feature (PF) dataset to facilitate these investigations. For example, this new dataset is being used to study the microphysical and dynamical response of the extratropical transition of tropical cyclones (TCs) [*Gatlin et al.*, 2019]. The changing thermodynamic structures of these cyclones are expected to manifest in the lightning and precipitation characteristics of these systems. ISS LIS is extremely important to this study since it enables inclusion of cyclones in the Pacific and Indian Oceans, and thus provides a more global perspective on the extratropical transition process. The ISS LIS-enriched PF database dates to 2017, and the number of ISS and orbital GPM coincidences continue to increase with time, which should soon enable meaningful statistics on the convective characteristics of mid-latitude-transitioning TCs.

4.3. LNO_x estimation for climate and air quality studies

Lightning produces nitrogen oxides (NO_x = NO + NO_2) that affects the concentration of greenhouse gases such as ozone [*Huntrieser et al.*, 1998; *Pickering et al.*, 2016]. Accurately characterizing trends in NO_x production is crucial for monitoring the composition of the atmosphere, as well as monitoring climate variability and change. Since climate is most sensitive to ozone in the upper troposphere, and since lightning is the most important source of NO_x in the upper troposphere at tropical and subtropical latitudes, lightning is a particularly useful parameter to monitor for climate assessments. Satellite-based optical lightning mappers have been used to make preliminary estimates of lightning NO_x (LNO_x) and used to examine long-term trends in annual production, as well as short-term interannual variability [*Koshak*, 2017]. Continuing these data records using ISS LIS observations is planned, and is particularly important for supporting the NCA program.

LNO_x also impacts ozone estimates made by regional air quality models [e.g., *Koshak et al.*, 2014a]. Hence a better understanding of the contribution of LNO_x to greenhouse gas pollution in the lower troposphere is needed. Also onboard the ISS is the Stratospheric Aerosol and Gas Experiment (SAGE) III [*Flittner et al.*, 2018], which provides observations of nitrogen dioxide (NO_2) that will provide ideal comparisons with ISS LIS retrievals of LNO_x. New geostationary instruments - Tropospheric Emissions: Monitoring of Pollution (TEMPO), Sentinel-4, and Geostationary Environment Monitoring Spectrometer (GEMS) - will provide unique NO_2 measurements [*Zoogman et al.*, 2017; *Courrèges-Lacoste et al.*, 2017; *Kim et al.*, 2020] for comparison with ISS LIS. This combination of satellite-based chemistry measurements together with ISS LIS offer an unprecedented opportunity to fully probe LNO_x production that is so vital to climate and air quality studies.

5. Summary and conclusions

ISS LIS has completed more than three years on orbit. During that time, it has met all of its major science objectives, including detection of lightning during day and night, at storm-scale (~4-km) spatial resolution, with millisecond timing and reasonably high flash detection efficiency (64% relative to a comparable optical sensor) without a land/ocean bias. ISS LIS also measures radiant energy, which though not discussed in depth in this paper is relevant to many studies such as NO_x generation by lightning [e.g., *Pickering et al.*, 2016] and differences in land/ocean flash characteristics [e.g., *Nag and Cummins*, 2017]. ISS LIS also provides background images/intensity, and delivers near-realtime lightning data. In addition, it has produced a lightning climatology that is fundamentally consistent with previous lightning climatologies, while also enabling the extension of the climatologies into the current era as well as to higher latitudes (± 55°). Global-scale flash rates (3-year average: ~44 s^{-1}) are within 5-10% of previous datasets [e.g., *Cecil et al.*, 2014], and the spatial and diurnal distributions of global lightning are consistent with expectations [e.g., *Blakeslee et al.*, 2014]. ISS LIS has demonstrated its value as a calibration/validation tool for current and future spaceborne lightning datasets. The near-realtime ISS LIS data have opened up applications within operational weather forecasting and related applications, including public safety. Finally, ISS LIS is demonstrating utility as part (or potential part) of cross-platform studies examining a diverse array of topics, including lightning physics, thunderstorm processes, convective precipitation, and atmospheric composition.

Appendix A. Other instrument/platform requirements

A.1 Successfully characterize the instrument's field of view (FOV)

The ISS LIS instrument has a 78.5° x 78.5° rectangular FOV imaged on a 128 x 128 pixel charge coupled device (CCD). At 400-km altitude this provides "storm-scale" pixel resolution (nadir) of ~4 km (and 50% larger at off-nadir boundaries), which is similar to TRMM LIS after its orbit boost in 2001. Obscuration of the FOV by ISS solar panels and radiator that periodically pass through the FOV was quantified. Worst-case mean and peak obscuration is 4% and 12.5%, respectively. Since ISS is a moving platform, small obstructions in the FOV will only lower view-time of a point on the ground (e.g., storm) momentarily, so there is no impact to science provided the view times are appropriately adjusted. Current version 1 ISS LIS data likely have a slight, artificially reduced (~1-2%) detection efficiency (DE) due to overestimates of viewing times. FOV analysis remains an ongoing process, and improved viewing time estimates are expected in version 2 ISS LIS data.

A.2 Mitigate solar glare/glint, and control the thermal and contamination environments

Reflection of direct sunlight into the sensor will not damage LIS, but sufficient glint signal has the potential to momentarily "blind" LIS by filling its first-in/first-out (FIFO) buffer. Pre-launch, Manipulator Analysis Graphics and Interactive Kinematics (MAGIK) analysis was performed by NASA Johnson Space Center (JSC) to assess potential glare/glint and its impact. No glare spots or rapidly changing illumination were detected from either the solar panels or radiator. Images obtained from nadir-viewing cameras in STP-H4 (another STP mission located close to ISS LIS) qualitatively corroborate this result. Analysis of numerous other ISS images and videos also supported this inference (not shown).

During mission development, STP-H5 and LIS engineers examined both survival (during transfer) and temperature exceedance during operation. It was found that on-orbit temperatures remained within acceptable limits. Realtime housekeeping data from ISS LIS, including relevant temperatures, are gathered and posted to an internal website. These data are regularly monitored to ensure nominal instrument performance.

Modeling analysis was conducted for the molecular contamination effects on the LIS window transmission at 777.4 nm. The modeling was based on previous flight data from materials exposed in the ISS environment and estimations of outgassing rates in that environment for the mission duration of 3 years. Values were taken from baseline external contamination assessments collected during pre-launch testing. Worst case scenario showed only a 5% decrease in absolute transmission over 3 years due to typical contaminates. However, no significant loss has been observed to date with ISS LIS, and the nearly identical TRMM LIS instrument showed very limited performance degradation over its 17-year life span [*Buechler et al.*, 2014].

A.3 Laboratory calibration

The laboratory calibration of TRMM LIS is discussed in detail in *Koshak et al.* [2000], and this was the same calibration approach applied to the spare LIS unit (i.e., ISS LIS). The calibration consisted of four main efforts: (1) a static response test, a (2) transient response test, (3) a spectral test, and (4) an FOV test. Additional elements of the calibration pertinent to LIS performance characteristics are discussed in *Boccippio et al.* [2002].

The calibration tests, which are referred to here as the original calibration (OC), were carried out on both the original TRMM LIS and the spare unit (the present ISS LIS) in the summer of 1997. TRMM LIS was subsequently launched to orbit, while the spare unit was stored in a safe box in an environmentally controlled facility for many years, until it was integrated on STP-H5. In the summer of 2014 and prior to the integration on STP-H5, a retest calibration (RC) was performed on the spare unit to determine if there were any significant changes in the OC given the many years that the unit was in storage. The RC instrumentation and procedures employed were made as similar as possible to those employed in the OC, but unfortunately the OC and RC methodologies were not identical.

A brief overview of the OC tests applied to both the TRMM LIS and ISS LIS are provided below:

- **Static Response Test**: The OC static response test provided the linear response of each pixel, and hence also quantified uniformity across the charge coupled device (CCD) array. It employed an 8-inch integrating sphere calibration standard. The sphere lamp source emitted a static radiance that was nearly isotropic and uniform over the 2-inch diameter exit port (source stability at 3000 K color temperature was specified at ± 0.5% over a 1-hr duration, and ± 2.0% over 100 hr). The radiance was continuously adjustable over a range of five orders of magnitude without changing the color temperature. Since the sphere output could not fill the sensor FOV, a motorized positioning system (containing precision Newport/Klinger rotation stages) was used to yaw and pitch the sensor head to effect full FOV coverage.

- **Transient Response Test**: The purpose of the OC transient response test was to determine the transient response of the sensor to optical pulses of various integrated energies, against several different levels of steady-state background radiance, and for several different pixels across the CCD array. Pulse energy was changed by varying the pulse duration within a 2-ms LIS frame. The primary component of the test system was a 2-inch integrating sphere containing a near-infrared light emitting diode (LED) and a small quartz tungsten halogen (QTH) lamp. The LED was mounted behind a pinhole in the far surface of the sphere. Background radiance levels were adjusted by a variable aperture in the lamp input port, thus maintaining a constant color temperature.
- **Spectral Response Test**: The OC spectral test employed a high-resolution grating monochromator (500-mm focal length, f/5 aperture, and 0.1-nm resolution) as the primary component. The attached source module contained a QTH lamp and a krypton rare gas discharge lamp as a wavelength reference. The monochromator output was fed through a fiber-optic cable whose output was approximately collimated by a small off-axis paraboloid mirror. By scanning in wavelength, the spectral test determined the sensor end-to-end relative spectral response. This test covered only the wavelength region near and within the passband of the narrowband interference filter.
- **FOV Test**: The FOV test in the OC employed a 9-inch diameter, off-axis paraboloid mirror and an infrared LED. The LED was used to illuminate a total of 31 pixels that were evenly spaced across the CCD, and the associated source incidence angles for each pixel was

computed. The LED incidence angles to the lens could be viewed equivalently as lightning source angles. The geometrical mappings were mathematically unique and were used to build a lens transfer function (i.e., boresight angle vs. pixel distance from center of the CCD). These results are fundamental to the process of geolocating lightning. The overall sensor FOV (approximately 78.5° x 78.5°) was determined by simply illuminating pixels on the CCD perimeter.

As mentioned previously, the RC methodology and equipment were not identical to the OC. In the fall of 2013, prior to beginning the RC, it was deemed necessary to upgrade much of the equipment employed in the OC, since these were out of date and were no longer compatible with current technology. For the static response test, two integrating sphere systems were procured. The first was a 12-inch sphere with a large aperture which was intended to allow uniform illumination of a larger portion of each quadrant of the ISS LIS instrument. The second was a 6-inch sphere that was comparable but not the same size as the 8-inch sphere used in the OC. This second sphere was acquired for the purposes of transient testing, as it had a removable port in the back for attaching an LED.

Ultimately the 12-inch sphere was deemed unusable for the static response test because the large opening allowed for “hotspots” where the luminosity was greater surrounding the tungsten bulbs. The 6-inch sphere worked for testing the static response of the instrument; however, it only covered a fraction of each of the quadrants. After comparing the results with the legacy calibration, it was noticed that there was a form factor difference, so the legacy 8-inch sphere was then used to determine if the values were still the same as the legacy calibration. Using the legacy sphere as a one-to-one comparison with the previous calibration was a success.

Use of the 6-inch sphere for transient testing was originally the plan; however, after inserting the newly painted LED insert there were noticeable differentials in the reflectivity of the new insert, especially around the edges. It was decided to use the LED as the source for the backgrounds for each pixel and then on top of that send the pre-programmed transient signal. This allowed for a very controllable and fluid process for the transient calibration.

For the spectral test, the grating monochromator used in the OC could no longer be used because the controller was no longer available, and the connections were obsolete. Instead, a new monochromator was employed for the RC. The FOV test for the RC was performed in much the same way as in the OC, and the results were essentially identical.

ISS LIS alignment measurements were conducted in the RC. The alignment measurements were obtained by illuminating different sides of a mirror-faced alignment cube (attached to the outside of the LIS sensor head assembly) with a theodolite; this allowed determination of the overall rigid alignment of the LIS lens/CCD systems with the STP-H5 module and ISS platform.

While the RC procedure was acceptable, it was not optimal. The intent of the RC was to ensure that nothing significantly changed with the instrument during the years in storage. For expediency, and because the RC results showed no significant changes from the OC results for TRMM LIS (Fig. A1), the OC results for the TRMM LIS were applied in the ISS LIS processing code, which produces the version 1 dataset available at the GHRC.

However, a plan is being implemented to replace the TRMM LIS OC results in the ISS LIS processing code with the ISS LIS OC results, since identical procedures could not be followed due to the passage of time. In particular, the RC static response test was incomplete because it did not cover all pixels in the CCD array; it only illuminated a small circular portion in the center of each quadrant. This leaves some lingering calibration uncertainties in the version 1 ISS LIS dataset. The ISS LIS science team is working to retrieve the digital OC calibration data for the spare unit, and before updating the ISS LIS processing code the ISS OC and RC results will be compared in detail, as well as with the OC results for TRMM LIS. Based on initial analysis, an improvement of 2-5% in key instrument performance parameters (e.g., flash detection efficiency, flash false alarm rate, geolocation accuracy, and optical amplitudes) is expected after a future switch to the ISS LIS OC.

Acknowledgements

ISS LIS resulted from and with several key partnerships. The ISS Program Research Integration Office (PRIO) at NASA Johnson Space Center (JSC) provided funding for development, launch and integration of LIS. The ISS PRIO also funded the DoD Space Test Program (STP) to add LIS to the STP-H5 Payload. The NASA Science Mission Directorate Earth Science Division initially leveraged TRMM LIS science funding to cover ISS LIS science, and then transitioned this support in 2017 to the Earth from ISS program. NASA Marshall Space Flight Center (MSFC) partnered with University of Alabama Huntsville (UAH) to prepare the spare LIS for ISS, which included building the new Interface Unit (IFU), and MSFC partnered with NASA Goddard Space Flight Center to build key fiber optic harnesses for LIS. The LIS Science Team gratefully acknowledges the productive science and operations collaborations between MSFC, UAH, STP, Universities Space Research Association (USRA), and the ISS Payload Operations Integration Center. ISS-LIS and STP-5 were launched to the ISS from Kennedy Space Center (KSC) after integration onto a SpaceX rocket. ISS LIS data are available from the GHRC DAAC via the Digital Object Identifiers (DOIs) listed in the *Blakeslee* [2019a-d] references. Extensive user support services, including Python-based recipes to analyze ISS LIS data, are also available [*GHRC*, 2020]. Anonymous reviewers and Earle Williams are thanked for their comments and suggestions to improve the manuscript.

References

Aich, V., R. Holzworth, S. J. Goodman, Y. Kuleshov, C. Price, and E. Williams, 2018: Lightning: A new essential climate variable, Eos, 99, https://doi.org/10.1029/2018EO104583.

Albrecht, R.I., S.J. Goodman, D.E. Buechler, R.J. Blakeslee, and H.J. Christian, 2016: Where Are the Lightning Hotspots on Earth?. Bull. Amer. Meteor. Soc., 97, 2051–2068, https://doi.org/10.1175/BAMS-D-14-00193.1

Bitzer, P. M. (2017), Global distribution and properties of continuing current in lightning, J. Geophys. Res. Atmos., 122, 1033– 1041, doi:10.1002/2016JD025532.

Bitzer, P.M., J.C. Burchfield, and H.J. Christian, 2016: A Bayesian Approach to Assess the Performance of Lightning Detection Systems. J. Atmos. Oceanic Technol., 33, 563–578, https://doi.org/10.1175/JTECH-D-15-0032.1

Bitzer, P.M. and H.J. Christian, 2015: Timing Uncertainty of the Lightning Imaging Sensor. J. Atmos. Oceanic Technol., 32, 453–460, https://doi.org/10.1175/JTECH-D-13-00177.1

Bitzer, P. M., Christian, H. J., Stewart, M., Burchfield, J., Podgorny, S., Corredor, D., Hall, J., Kuznetsov, E., and Franklin, V. (2013), Characterization and applications of VLF/LF source locations from lightning using the Huntsville Alabama Marx Meter Array, J. Geophys. Res. Atmos., 118, 3120– 3138, doi:10.1002/jgrd.50271.

Blakeslee, Richard J., 2019a. NRT Lightning Imaging Sensor (LIS) on International Space Station (ISS) Science Data. Dataset available online from the NASA Global Hydrology Resource Center DAAC, Huntsville, Alabama, U.S.A. http://dx.doi.org/10.5067/LIS/ISSLIS/DATA106.

Blakeslee, Richard J., 2019b. NRT Lightning Imaging Sensor (LIS) on International Space Station (ISS) Backgrounds. Dataset available online from the NASA Global Hydrology Resource Center DAAC, Huntsville, Alabama, U.S.A. http://dx.doi.org/10.5067/LIS/ISSLIS/DATA206.

Blakeslee, Richard J., 2019c. Non-Quality Controlled Lightning Imaging Sensor (LIS) on International Space Station (ISS) Science Data. Dataset available online from the NASA Global Hydrology Resource Center DAAC, Huntsville, Alabama, U.S.A. http://dx.doi.org/10.5067/LIS/ISSLIS/DATA107.

Blakeslee, Richard J., 2019d. Non-Quality Controlled Lightning Imaging Sensor (LIS) on International Space Station (ISS) Backgrounds. Dataset available online from the NASA Global Hydrology Resource Center DAAC, Huntsville, Alabama, U.S.A. http://dx.doi.org/10.5067/LIS/ISSLIS/DATA207.

Blakeslee, R. J., Mach, D. M., Bateman, M. G., & Bailey, J. C. (2014). Seasonal variations in the lightning diurnal cycle and implications for the global electric circuit. Atmospheric research, 135, 228-243.

Boccippio, D. J., W. J. Koshak, R. J. Blakeslee, 2002: Performance assessment of the Optical Transient Detector and Lightning Imaging Sensor. Part I: predicted diurnal variability, J. Atmos. Oceanic Technol., 19, 1318-1332.

Bruning, E., Tillier, C. E., Edgington, S. F., Rudlosky, S. D., Zajic, J., Gravelle, C., et al. (2019). Meteorological imagery for the geostationary lightning mapper. Journal of Geophysical Research: Atmospheres, 2019; 124: 14285– 14309. https://doi.org/10.1029/2019JD030874

Buechler, D. E., Koshak, W. J., Christian, H. J., & Goodman, S. J. (2014). Assessing the performance of the Lightning Imaging Sensor (LIS) using deep convective clouds. Atmospheric research, 135, 397-403.

Cecil, D. J., Buechler, D. E., & Blakeslee, R. J. (2014). Gridded lightning climatology from TRMM-LIS and OTD: Dataset description. Atmospheric Research, 135, 404-414.

Chanrion, O., Neubert, T., Lundgaard Rasmussen, I. et al. The Modular Multispectral Imaging Array (MMIA) of the ASIM Payload on the International Space Station. Space Sci Rev 215, 28 (2019). https://doi.org/10.1007/s11214-019-0593-y

Christian, H. J., Blakeslee, R. J., and Goodman, S. J. (1989), The detection of lightning from geostationary orbit, J. Geophys. Res., 94(D11), 13329– 13337, doi:10.1029/JD094iD11p13329.

Christian, H. J., et al., Global frequency and distribution of lightning as observed from space by the Optical Transient Detector, J. Geophys. Res., 108(D1), 4005, doi:10.1029/2002JD002347, 2003.

Christian, H. J., R. L. Frost, P. H. Gillaspy, S. J. Goodman, O. H. Vaughan, M. Brook, B. Vonnegut, and R. E. Orville (1983), Observations of optical lightning emissions from above thunderstorms using U−2 aircraft, Bull. Am. Meteorol. Soc., 64, 120–123. doi: 0.1175/1520-0477(1983)064<0120:OOOLEF>2.0.CO;2.

Courrèges-Lacoste, G. B. M. Sallusti, G. Bulsa, G. Bagnasco, Ben Veihelmann, S. Riedl, D. J. Smith, R. Maurer, 2017: The Copernicus Sentinel 4 mission: a geostationary imaging UVN spectrometer for air quality monitoring, Proc. SPIE 10423, Sensors, Systems, and Next-Generation Satellites XXI, 1042307. doi: 10.1117/12.2282158

Darden, C.B., D.J. Nadler, B.C. Carcione, G.T. Stano, and D.E. Buechler, 2009: Utilizing total lightning information to diagnose convective trends. Bull. Amer. Meteor. Soc., 91, 167-175. doi: http://dx.doi.org/10.1175/2009BAMS2808.1

Earthdata, cited 2020. NASA Earthdata Search. [Available online at https://search.earthdata.nasa.gov/.]

Erdmann, F., Defer, E., Caumont, O., Blakeslee, R. J., Pédeboy, S., and Coquillat, S.: Concurrent satellite and ground-based lightning observations from the Optical Lightning Imaging Sensor (ISS-LIS), the low-frequency network Meteorage and the SAETTA Lightning Mapping Array (LMA) in the northwestern Mediterranean region, Atmos. Meas. Tech., 13, 853–875, doi: 10.5194/amt-13-853-2020, 2020.

Evans, C., S. Shrestha, E. Raphael, J. Luvall, R. Griffin, and P. Gatlin, 2018: Hindu-Kush Himalayan Disasters. Integrating NASA Earth observations to monitor intense thunderstorms and assess lightning exposure and risk in the Hindu-Kush Himalayan region. NASA DEVELOP Technical Report., 19 pp.

Flittner, D., Thomason, L., Hill, C., Roell, M., Pitts, M., Damadeo, R., ... & Stanley, R. (2018, April). Stratospheric Aerosol and Gas Experiment III installed on the International Space Station (SAGE III/ISS): Overview. In EGU General Assembly Conference Abstracts (Vol. 20, p. 5483).

Gatlin, P., L. Huescher, C. Liu, W. Petersen, D. J. Cecil, 2019: The evolution and extratropical transition of tropical cyclones from a GPM, ISS LIS and GLM perspective, AGU 2019 Fall Meeting, December 9-13, 2019, San Francisco, CA, American Geophysical Union, H13P-1976.

Global Hydrology Resource Center, cited 2020. ISS LIS Lightning Flash Location Quickview using Python 3.0 and GIS. [Available online at https://ghrc.nsstc.nasa.gov/home/data-recipes/iss-lis-lightning-flash-location-quickview-using-python-30-and-gis].

Goodman, S. J., R. J. Blakeslee, W. J. Koshak, D. Mach, J. Bailey, D. Buechler, L. Carey, C. Schultz, M. Bateman, E. McCaul, G. Stano, The GOES-R Geostationary Lightning Mapper (GLM), Atmospheric Research, Volumes 125–126, 2013, Pages 34-49, ISSN 0169-8095, https://doi.org/10.1016/j.atmosres.2013.01.006.

Goodman, S. J., R. J. Blakeslee, B. P. Pettegrew, A. Terborg, S. N. Stevenson, M. J. Folmer, S. S. Lindstrom, G. T. Stano, S. G. Harrison, and K. S. Virts, 2020a: NWS Use of Near Real-Time Lightning Data from the Lightning Imaging Sensor (LIS) on the International Space Station (ISS), Poster 1478, Annual Meeting, Amer. Meteorol. Soc., Boston, MA.

S. J. Goodman, R. J. Blakeslee, B. P. Pettegrew, A. Terborg, M. J. Folmer, S. N. Stevenson, K. S. Virts, and J. W. Smith, 2020b: NWS Complementary Use of the Geostationary Lightning Mapper (GLM) and Lightning Imaging Sensor (LIS), JPSS/GOES-R Proving Ground/Risk Reduction Summit [Available online at https://www.star.nesdis.noaa.gov/star/documents/meetings/2020JPSSGOES/Posters/B_2_JPSS-GOESR_PGRR_Summit_Poster_FINAL_sgoodman.pdf]

Hou, A.Y., Kakar, R.K., Neeck, S., Azarbarzin, A.A., Kummerow, C.D., Kojima, M., Oki, R., Nakamura, K. and Iguchi, T. (2014) The global precipitation measurement mission. Bulletin of the American Meteorological Society, 95, 701–722. doi:10.1175/BAMS−D−13−00164.1.

Hui, W., F. Huang and R. Liu (2020) Characteristics of lightning signals over the Tibetan Plateau and the capability of FY-4A LMI lightning detection in the Plateau, International Journal of Remote Sensing, 41, 4605-4625, doi: 10.1080/01431161.2020.1723176.

Huntrieser, H., Schlager, H., Feigl, C., and Höller, H. (1998), Transport and production of NO X in electrified thunderstorms: Survey of previous studies and new observations at midlatitudes, J. Geophys. Res., 103(D21), 28247– 28264, doi:10.1029/98JD02353.

HyDRO, cited 2020. NASA Hydrology Data Search Tool. [Available online at https://ghrc.nsstc.nasa.gov/hydro.]

ISS LIS, cited 2020. ISS LIS Datasets. [Available online at https://ghrc.nsstc.nasa.gov/lightning/data/data_lis_iss.html.]

Jacobson, A. R., Light, T. E. L., Hamlin, T., and Nemzek, R.: Joint radio and optical observations of the most radio-powerful intracloud lightning discharges, Ann. Geophys., 31, 563–580, https://doi.org/10.5194/angeo-31-563-2013, 2013.

Jedlovec, G., 2013: Transitioning research satellite data to the operational weather community: The SPoRT paradigm. IEEE Geoscience and Remote Sensing Magazine, 1, no. 1, 62–66, https://doi.org/10.1109/MGRS.2013.2244704.

Kim, J. and Coauthors, 2020: New era of air quality monitoring from space: Geostationary Environment Monitoring Spectrometer (GEMS). Bull. Amer. Meteor. Soc., E1-E22. doi: 10.1175/ BAMS-D-18-0013.1.

P. Kokou et al., "Algorithmic Chain for Lightning Detection and False Event Filtering Based on the MTG Lightning Imager," in IEEE Transactions on Geoscience and Remote Sensing, vol. 56, no. 9, pp. 5115-5124, Sept. 2018, doi: 10.1109/TGRS.2018.2808965.

Koshak, W. (2017). Lightning-Related Indicators for National Climate Assessment (NCA) Studies. Fall Meeting 2017, American Geophysical Union, New Orleans, LA.

Koshak, W. J., K. L. Cummins, D. E. Buechler, B. Vant-Hull, R. J. Blakeslee, E. R. Williams, H. S. Peterson, 2015: Variability of CONUS Lightning in 2003-12 and Associated Impacts, J. Appl. Meteorol. Climatology, 54, No. 1, 15-41.

Koshak, W. J., B. Vant-Hull, E. W. McCaul, and H. S. Peterson, Variation of a lightning NOx indicator for national climate assessment, XV International Conference on Atmospheric Electricity, Norman, Oklahoma, June 15-20, 2014a.

Koshak, W. J., H. S. Peterson, A. P. Biazar, M. N. Khan, and L. Wang, 2014b: The NASA Lightning Nitrogen Oxides Model (LNOM): Application to air quality modeling, Atmos. Res., 135-136, 363-369, doi:10.1016/j.atmosres.2012.12.015.

Koshak, W. J., M. F. Stewart, H. J. Christian, J. W. Bergstrom, J. M. Hall, and R. J. Solakiewicz, 2000: Laboratory Calibration of the Optical Transient Detector and the Lightning Imaging Sensor, J. Atmos. Oceanic Technol., 17, 905-915.

Kummerow, C., W. Barnes, T. Kozu, J. Shiue, and J. Simpson, 1998: The Tropical Rainfall Measuring Mission (TRMM) Sensor Package. J. Atmos. Oceanic Technol., 15, 809–817, https://doi.org/10.1175/1520-0426(1998)015<0809:TTRMMT>2.0.CO;2

Lavigne, T., Liu, C., & Liu, N. (2019). How does the trend in thunder days relate to the variation of lightning flash density? Journal of Geophysical Research: Atmospheres, 124, 4955-4974. https://doi.org/10.1029/2018JD029920

Lefeuvre, F., Blanc, E., Pinçon, J. et al. TARANIS—A Satellite Project Dedicated to the Physics of TLEs and TGFs. Space Sci Rev 137, 301–315 (2008). doi: 10.1007/s11214-008-9414-4.

Liu, C., Cecil, D. J., Zipser, E. J., Kronfeld, K., and Robertson, R. (2012), Relationships between lightning flash rates and radar reflectivity vertical structures in thunderstorms over the tropics and subtropics, J. Geophys. Res., 117, D06212, doi:10.1029/2011JD017123.

Liu, F., Zhu, B., Lu, G., Qin, Z., Lei, J., Peng, K.−M., et al. (2018). Observations of blue discharges associated with negative narrow bipolar events in active deep convection. Geophysical Research Letters, 45, 2842– 2851. doi: 10.1002/2017GL076207.

Mach, D. M., Blakeslee, R. J., and Bateman, M. G. (2011), Global electric circuit implications of combined aircraft storm electric current measurements and satellite−based diurnal lightning statistics, J. Geophys. Res., 116, D05201, doi:10.1029/2010JD014462.

Mach, D. M., R. J. Blakeslee, M. G. Bateman, and J. C. Bailey, Electric fields, conductivity, and estimated currents from aircraft overflights of electrified clouds, J. Geophys. Res., 114, D10204, DOI:10.1029/2008JD011495, 2009.

Mach, D. M., R. J. Blakeslee, M. G. Bateman, and J. C. Bailey, Comparisons of total currents based on storm location, polarity, and flash rates derived from high altitude aircraft overflights, J. Geophys. Res., 115, D03201, DOI:10.1029/2009JD012240, 2010.

Mach, D. M., Christian, H. J., Blakeslee, R. J., Boccipio, D. J., Goodman, S. J., and Boeck, W. L. (2007), Performance assessment of the Optical Transient Detector and Lightning Imaging Sensor, J. Geophys. Res., 112, D09210, doi:10.1029/2006JD007787.

Marchand, M., Hilburn, K., & Miller, S. D. (2019). Geostationary lightning mapper and Earth networks lightning detection over the contiguous United States and dependence on flash characteristics. Journal of Geophysical Research: Atmospheres, 124, 11552– 11567. https://doi.org/10.1029/2019JD031039

Medici, G., K. L. Cummins, D. J. Cecil, W. J. Koshak, and S. D. Rudlosky, 2017: The intracloud lightning fraction in the contiguous United States. Mon. Wea. Rev., 145, 4481–4499, doi: 10.1175/MWR-D-16-0426.1.

Nag, A., and Cummins, K. L. (2017), Negative first stroke leader characteristics in cloud‐to‐ground lightning over land and ocean, Geophys. Res. Lett., 44, 1973– 1980, doi:10.1002/2016GL072270.

Neubert, T., Østgaard, N., Reglero, V. et al. The ASIM Mission on the International Space Station. Space Sci Rev 215, 26 (2019). doi: 10.1007/s11214-019-0592-z.

Noble, C. M. M., Beasley, W. H., Postawko, S. E., and Light, T. E. L. (2004), Coincident observations of lightning by the FORTE photodiode detector, the New Mexico Tech Lightning Mapping Array and the NLDN during STEPS, Geophys. Res. Lett., 31, doi: 10.1029/2003GL018989.

Østgaard, N., Gjesteland, T., Carlson, B. E., Collier, A. B., Cummer, S. A., Lu, G., and Christian, H. J. (2013), Simultaneous observations of optical lightning and terrestrial gamma ray flash from space, Geophys. Res. Lett., 40, 2423– 2426, doi:10.1002/grl.50466.

Peterson, M., & Rudlosky, S. (2019). The time evolution of optical lightning flashes. Journal of Geophysical Research: Atmospheres, 124, 333– 349. https://doi.org/10.1029/2018JD028741

Peterson, M., Rudlosky, S., & Deierling, W. (2017). The evolution and structure of extreme optical lightning flashes. Journal of Geophysical Research: Atmospheres, 122, 13,370– 13,386. https://doi.org/10.1002/2017JD026855

Petersen, W.A. and S.A. Rutledge, 2001: Regional Variability in Tropical Convection: Observations from TRMM. J. Climate, 14, 3566–3586, https://doi.org/10.1175/1520-0442(2001)014<3566:RVITCO>2.0.CO;2

Pickering, K. E., Bucsela, E., Allen, D., Ring, A., Holzworth, R., and Krotkov, N. (2016), Estimates of lightning NOx production based on OMI NO2 observations over the Gulf of Mexico, J. Geophys. Res. Atmos., 121, 8668– 8691, doi:10.1002/2015JD024179.

Rison, W., Krehbiel, P., Stock, M. et al. Observations of narrow bipolar events reveal how lightning is initiated in thunderstorms. Nat Commun 7, 10721 (2016). doi: 10.1038/ncomms10721.

Rudlosky, S. D., Goodman, S. J., Virts, K. S., & Bruning, E. C. (2019). Initial geostationary lightning mapper observations. Geophysical Research Letters, 46, 1097–1104. https://doi.org/10.1029/2018GL081052

Rudlosky, S.D., M.J. Peterson, and D.T. Kahn, 2017: GLD360 Performance Relative to TRMM LIS. J. Atmos. Oceanic Technol., 34, 1307–1322, https://doi.org/10.1175/JTECH-D-16-0243.1

Saunders, C., 2008: Charge separation mechanisms in clouds, Space Sci. Rev., 137, 335-353, doi 10.1007/s11214-008-9345-0.

Skofronick‐Jackson, G, Kirschbaum, D, Petersen, W, et al. The Global Precipitation Measurement (GPM) mission's scientific achievements and societal contributions: reviewing four years of advanced rain and snow observations. Q J R Meteorol Soc 2018; 144, 27–48. doi: 10.1002/qj.3313

Suszcynsky, D. M., Kirkland, M. W., Jacobson, A. R., Franz, R. C., Knox, S. O., Guillen, J. L. L., and Green, J. L. (2000), FORTE observations of simultaneous VHF and optical emissions from lightning: Basic phenomenology, J. Geophys. Res., 105, 2191–2201, doi:10.1029/1999JD900993.

Thomas, R. J., Krehbiel, P. R., Rison, W., Hamlin, T., Boccippio, D. J., Goodman, S. J., and Christian, H. J.: Comparison of ground-based 3-dimensional lightning mapping observations with satellite-based LIS observations in Oklahoma, Geophys. Res. Lett., 27, 1703–1706, doi: 10.1029/1999GL010845, 2000.

Ushio, T., S. Heckman, K. Driscoll, D. Boccippio, H. Christian, and Z. I. Kawasaki, 2002: Cross-sensor comparison of the Lightning Imaging Sensor (LIS), International Journal of Remote Sensing, 23, 2703-2712, doi: 10.1080/01431160110107789.

Veraverbeke, S., Rogers, B., Goulden, M. et al. Lightning as a major driver of recent large fire years in North American boreal forests. Nature Clim Change 7, 529–534 (2017). https://doi.org/10.1038/nclimate3329

Virts, K.S. and S.J. Goodman, 2020: Prolific Lightning and Thunderstorm Initiation over the Lake Victoria Basin in East Africa. Mon. Wea. Rev., https://doi.org/10.1175/MWR-D-19-0260.1

Virts, K.S., J.M. Wallace, M.L. Hutchins, and R.H. Holzworth, 2013: Highlights of a New Ground-Based, Hourly Global Lightning Climatology. Bull. Amer. Meteor. Soc., 94, 1381–1391, https://doi.org/10.1175/BAMS-D-12-00082.1

Williams, E.R., 1994: Global Circuit Response to Seasonal Variations in Global Surface Air Temperature. Mon. Wea. Rev., 122, 1917–1929, https://doi.org/10.1175/1520-0493(1994)122<1917:GCRTSV>2.0.CO;2

Williams, E. R. (2020). Lightning and climate change. *Lightning interaction with power systems Volume 1: Fundamentals and modelling*, A. Pantini, ed., The Institution of Engineering and Technology, 1-45.

Yoshida, S., T. Adachi, K. Kusunoki, S. Hayashi, T. Wu, T. Ushio, and E. Yoshikawa, 2017: Relationship between thunderstorm electrification and storm kinetics revealed by phased array weather radar, J. Geophys. Res. Atmos., 122, 3821–3836, doi:10.1002/ 2016JD025947.

Zhang, D., & Cummins, K. L. (2020). Time evolution of satellite−based optical properties in lightning flashes, and its impact on GLM flash detection. Journal of Geophysical Research: Atmospheres, 125, e2019JD032024. doi: 10.1029/2019JD032024

Zhang, D., K.L. Cummins, P. Bitzer, and W.J. Koshak, 2019: Evaluation of the Performance Characteristics of the Lightning Imaging Sensor. J. Atmos. Oceanic Technol., 36, 1015–1031, https://doi.org/10.1175/JTECH-D-18-0173.1

Zhu, Y., Bitzer, P., Stewart, M., Podgorny, S., Corredor, D., Burchfield, J., et al. (2020). Huntsville Alabama Marx Meter Array 2: Upgrade and capability. Earth and Space Science, 7, e2020EA001111.https://doi.org/10.1029/2020EA001111

Zoogman, P. and Coauthors, 2017: Tropospheric Emissions: Monitoring of Pollution (TEMPO), J. Quant. Spectrosc. Ra., 186, 17-39. doi: 10.1016/j.jqsrt.2016.05.008.

1066

Tables

Table 1. ISS LIS global flash rate (s^{-1}) versus the monthly smoothed TRMM LIS/OTD climatology [*Cecil et al.*, 2014].

Region	Annual	MAM	JJA	SON	DJF
TRMM LIS/OTD < 55°	45.9	45.9	54.3	48.2	35.6
ISS LIS < 55°	43.8	45.1	53.5	45.6	30.8
TRMM LIS/OTD < 38°	41.8	43.4	43.4	46.2	34.7
ISS LIS < 38°	39.5	42.8	41.0	43.8	30.3

Figure Captions

Figure 1. Visualization of the ISS LIS instrument, its location on the ISS, as well as its data collection, processing, and distribution.

Figure 2. Basic workflow showing the data processing of initial observations at the ISS through ground processing by GHRC and the LIS science team, to publication for end users.

Figure 3. Left: ISS LIS temporal offset relative to ENGLN, GLD360, GLM-16, and GLM-17. Right: ISS LIS spatial geolocation offset relative to these comparison datasets.

Figure 4. Top: Time series of peak temporal offset between ISS LIS and three different reference datasets (ENGLN, GLD360, and GLM-16). Middle: Time series of the modal peak of the spatial offset between ISS LIS and these reference datasets. Bottom: Time series of ISS LIS DE and FAR relative to the reference datasets.

Figure 5. ISS LIS flash detection efficiency as a function of local time of day, relative to GLM, ENGLN, and GLD360. Analysis period for ENGLN and GLD360 was 1 March 2017 through 31 December 2019. The period of analysis for GLM-16 was 20 December 2017 to 31 December 2019, and for GLM-17 it was 13 November 2018 to 31 December 2019 (i.e., after each satellite moved to the GOES-East and -West positions, respectively).

Figure 6. a) Three-year (March 2017 through February 2020) climatology of global lightning from ISS LIS. b) Post-boost climatology of lightning from TRMM LIS (September 2001 through December 2014).

Figure 7. Monthly time series of global lightning flash rate (between ± 38° latitude) from TRMM LIS and ISS LIS.

Figure 8. ISS LIS lightning climatology, broken out seasonally. a) March-May. b) June-August. c) September-November. d) December-February.

Figure 9. ISS LIS diurnal variability of global lightning flash rate, including land/ocean breakdown. a) Adjusted to local solar time. b) UTC time.

Figure 10. GLM-16 flash DE with respect to ISS LIS (left), ENGLN (middle), and GLD360 (right).

Figure 11. Lightning risk analysis for Nepal and Bangladesh, based on a combination of LIS flash rates and socioeconomic factors.

Figure 12. Comparison of ASIM and ISS LIS observations of a lightning flash over Madagascar. (top) an image of the lightning flash captured by the ASIM camera with ISS LIS events from the group closest in time to the frame (i.e., black line in bottom panel) plotted as green symbols whose size correspond to the radiance measured by the LIS camera and scaled (10^{-4}) to match

the same units of ASIM radiance, which are given in logarithmic scale to enhance the illuminated pixels. (bottom) time-series of ASIM 777.4 nm photometer (red) and LIS groups (green) with the shaded region corresponding to the duration of the ASIM camera frame.

Figure A1. The close comparison between the original TRMM LIS calibration (OC; labeled TRMM) and the retest calibration (RC) of ISS LIS (labeled ISS). for a representative subset of the instrument's FOV. Left: Static Response Test. Right: Transient Response Test.

Figures

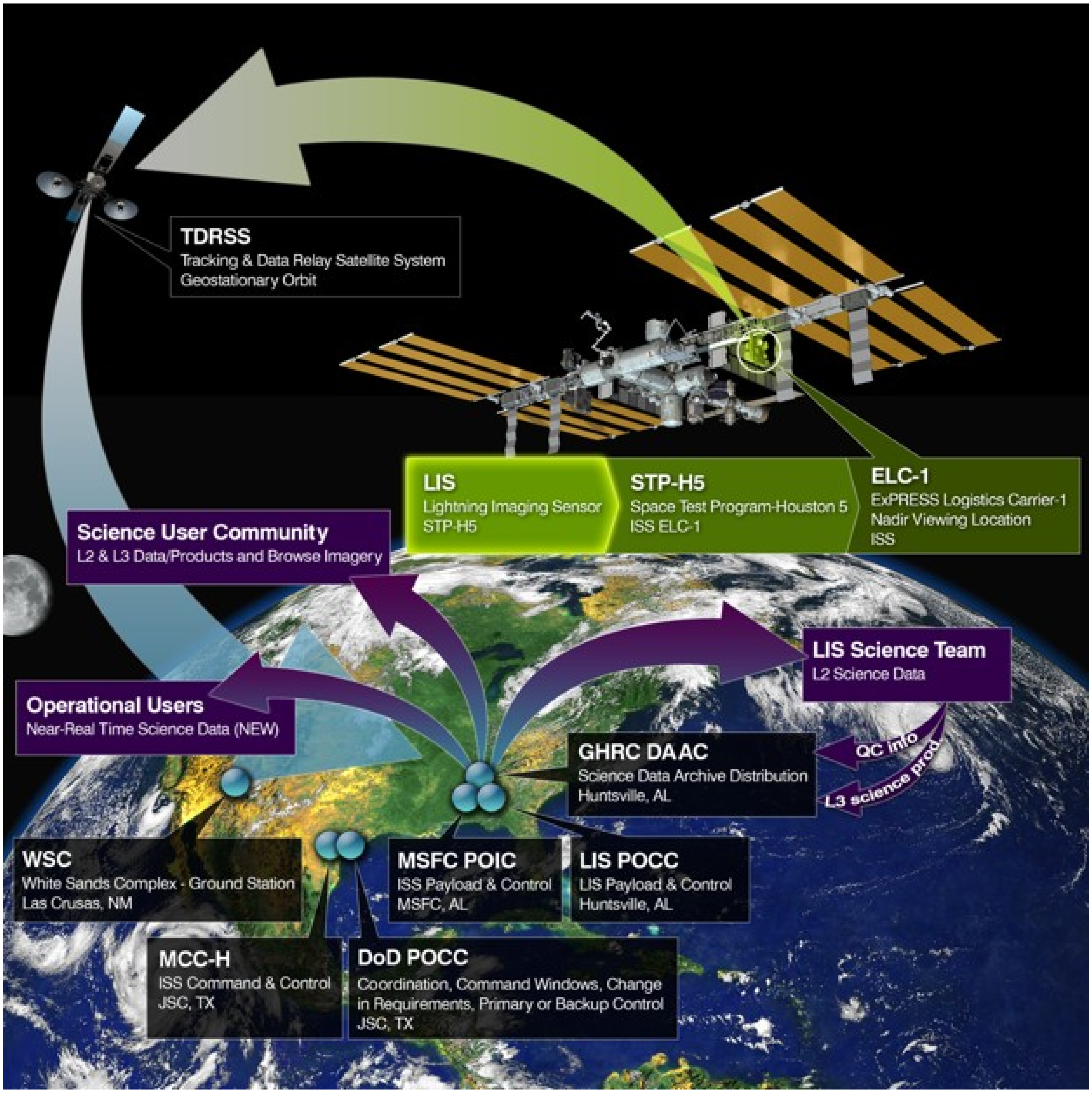

Figure 1. Visualization of the ISS LIS instrument, its location on the ISS, as well as its data collection, processing, and distribution.

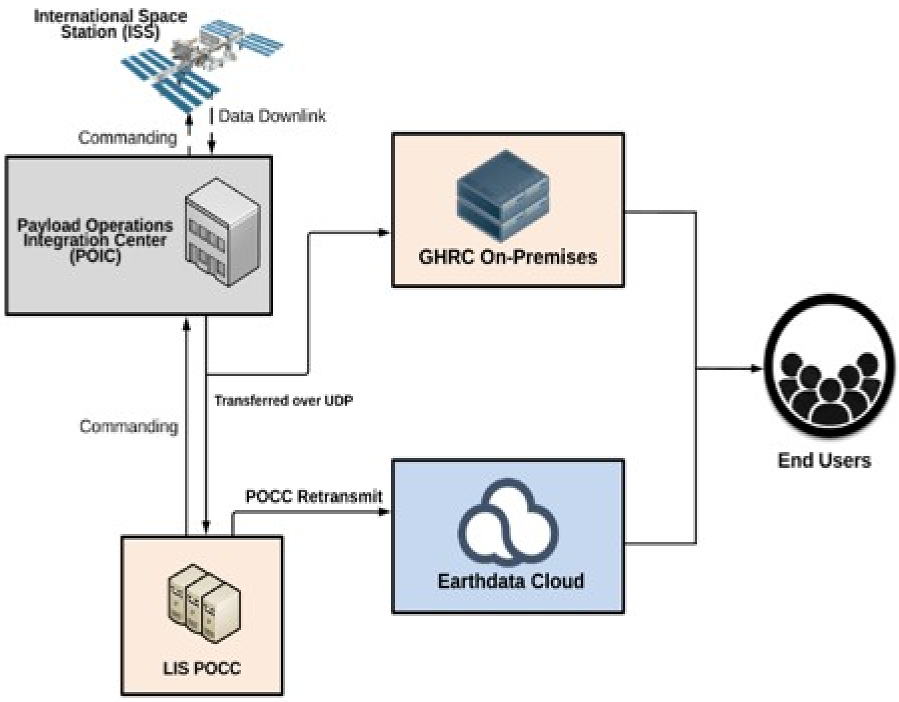

Figure 2. Basic workflow showing the data processing of initial observations at the ISS through ground processing by GHRC and the LIS science team, to publication for end users.

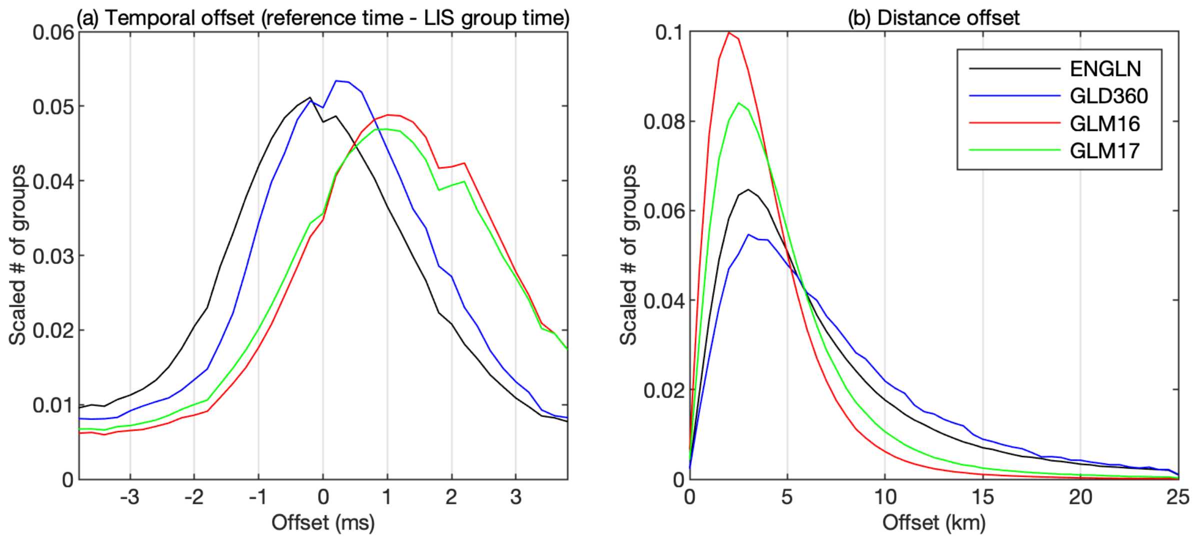

Fig. 3. Left: ISS LIS temporal offset relative to ENGLN, GLD360, GLM-16, and GLM-17. Right: ISS LIS spatial geolocation offset relative to these comparison datasets.

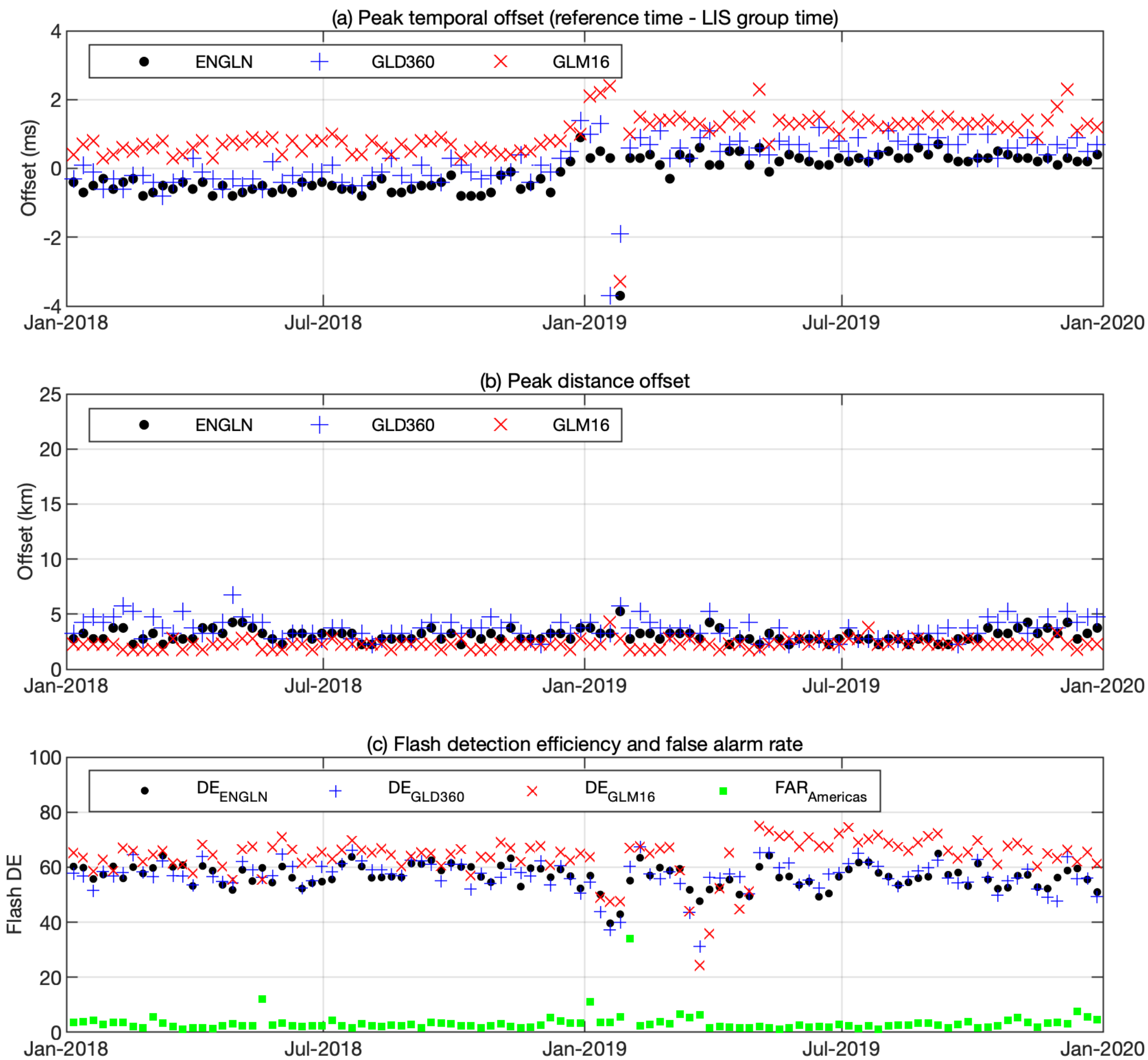

Figure 4. Top: Time series of peak temporal offset between ISS LIS and three different reference datasets (ENGLN, GLD360, and GLM-16). Middle: Time series of the modal peak of the spatial offset between ISS LIS and these reference datasets. Bottom: Time series of ISS LIS DE and FAR relative to the reference datasets.

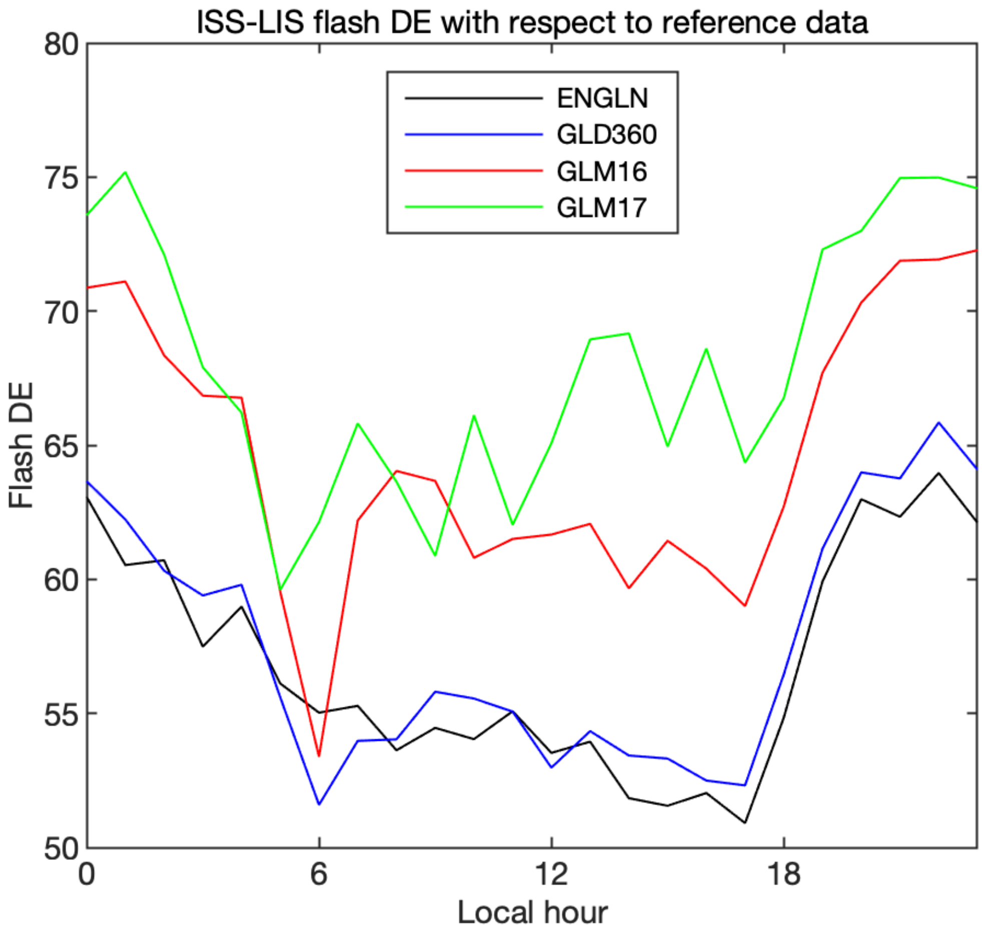

Figure 5. ISS LIS flash detection efficiency as a function of local time of day, relative to GLM, ENGLN, and GLD360. Analysis period for ENGLN and GLD360 was 1 March 2017 through 31 December 2019. The period of analysis for GLM-16 was 20 December 2017 to 31 December 2019, and for GLM-17 it was 13 November 2018 to 31 December 2019 (i.e., after each satellite moved to the GOES-East and -West positions, respectively).

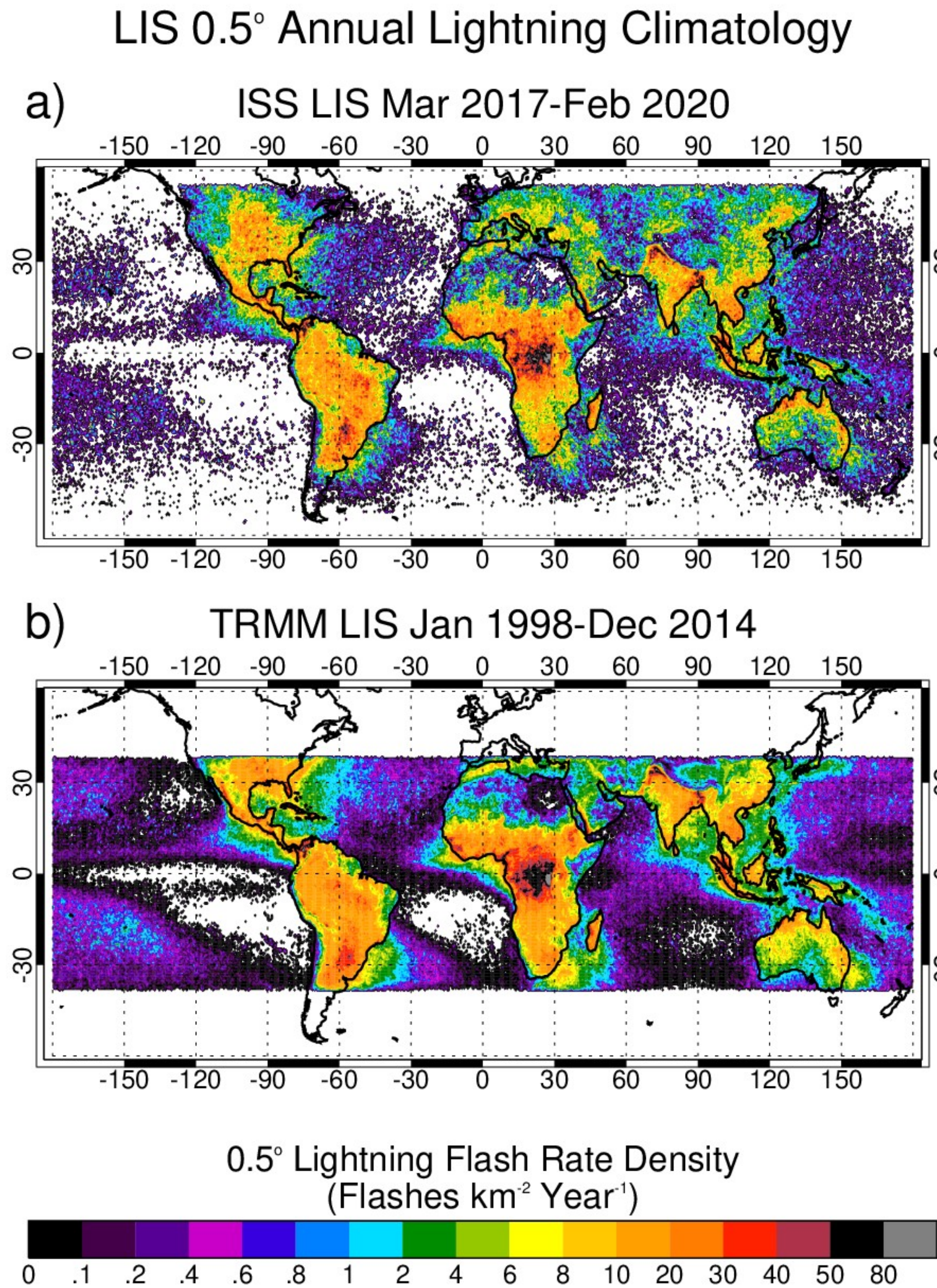

Figure 6. a) Three-year (March 2017 through February 2020) climatology of global lightning from ISS LIS. b) Post-boost climatology of lightning from TRMM LIS (September 2001 through December 2014).

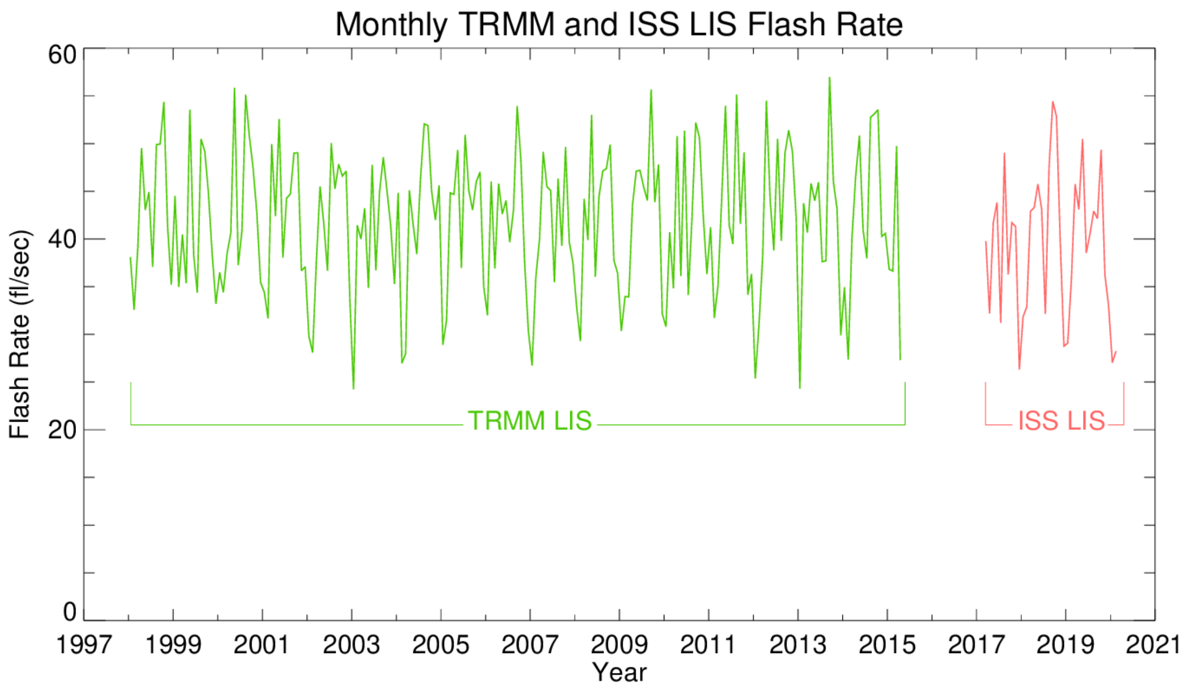

Figure 7. Monthly time series of global lightning flash rate (between ± 38° latitude) from TRMM LIS and ISS LIS.

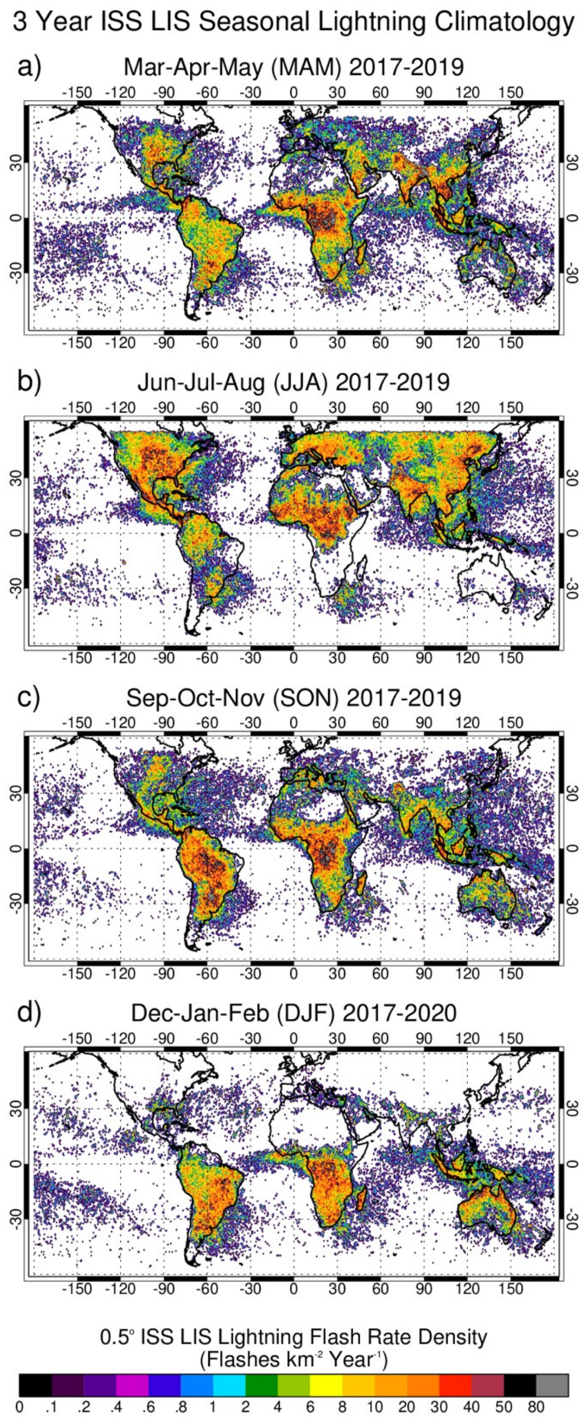

Figure 8. ISS LIS lightning climatology, broken out seasonally. a) March-May. b) June-August. c) September-November. d) December-February.

(Reviewers: Please see original figure to obtain full resolution)

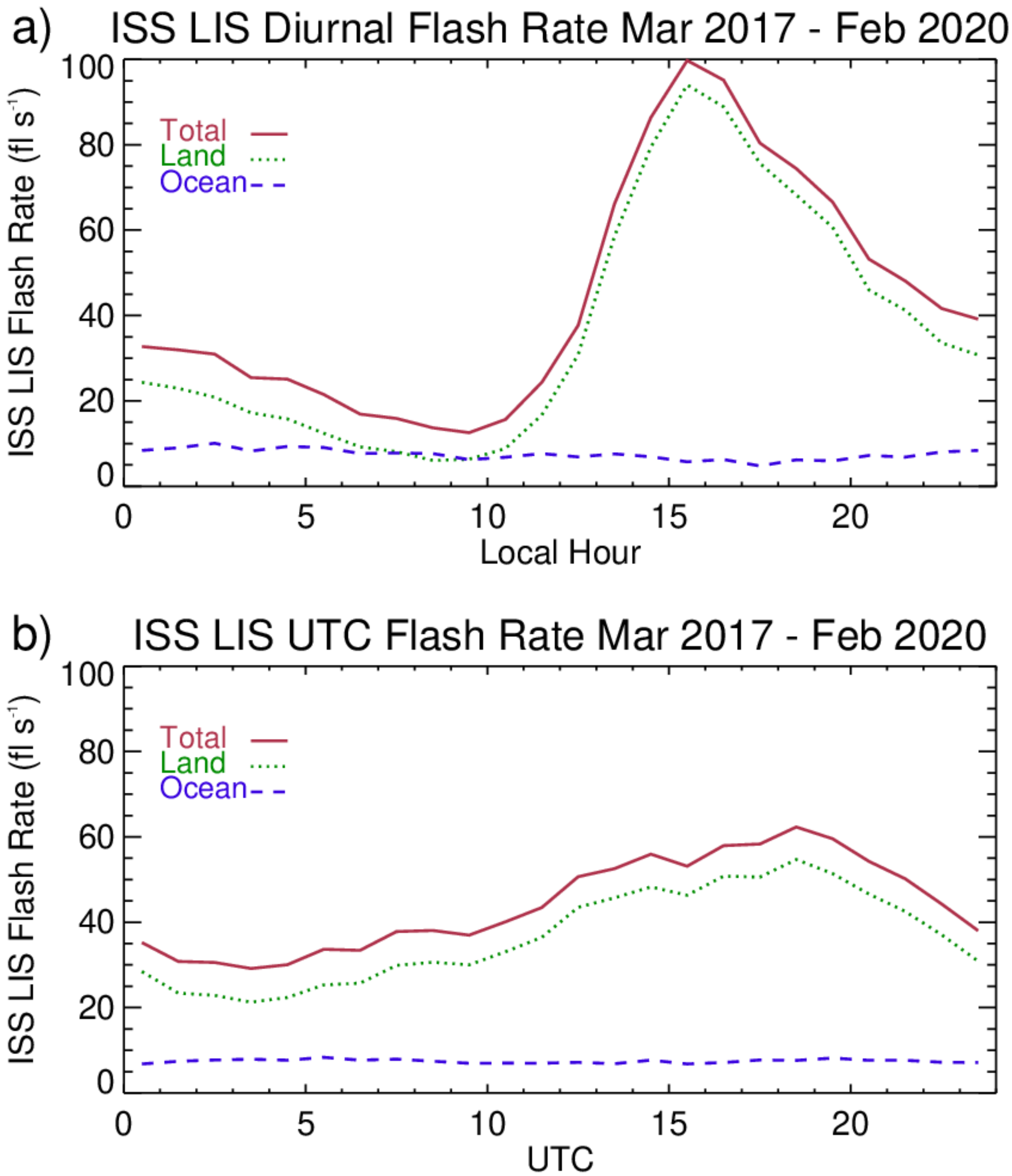

Figure 9. ISS LIS diurnal variability of global lightning flash rate, including land/ocean breakdown. a) Adjusted to local solar time. b) UTC time.

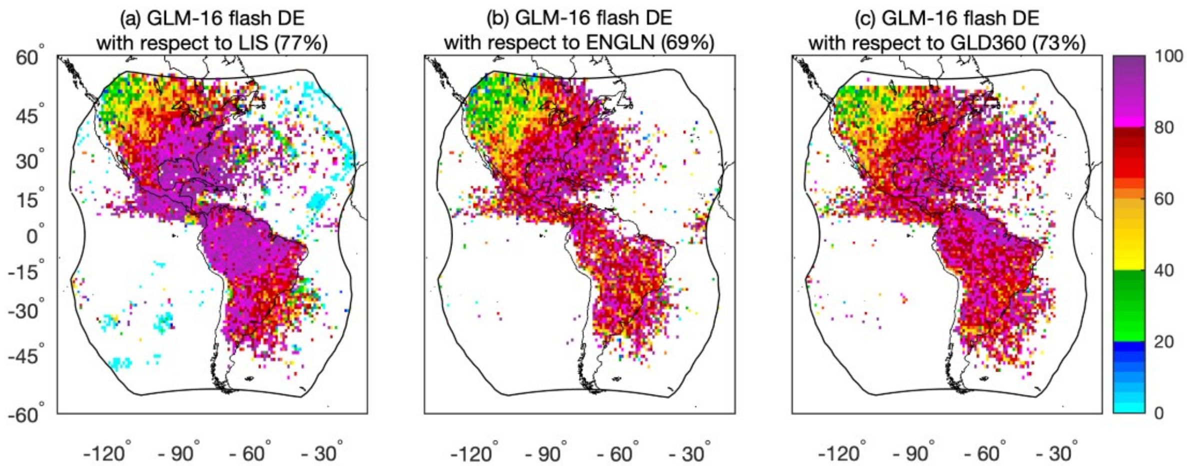

Figure 10. GLM-16 flash DE with respect to ISS LIS (left), ENGLN (middle), and GLD360 (right).

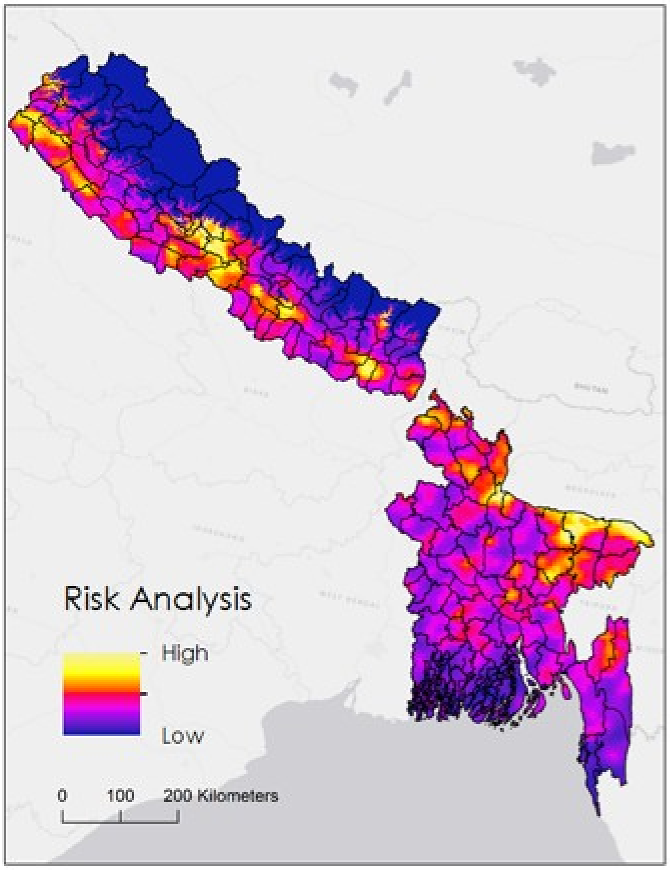

Figure 11. Lightning risk analysis for Nepal and Bangladesh, based on a combination of LIS flash rates and socioeconomic factors.

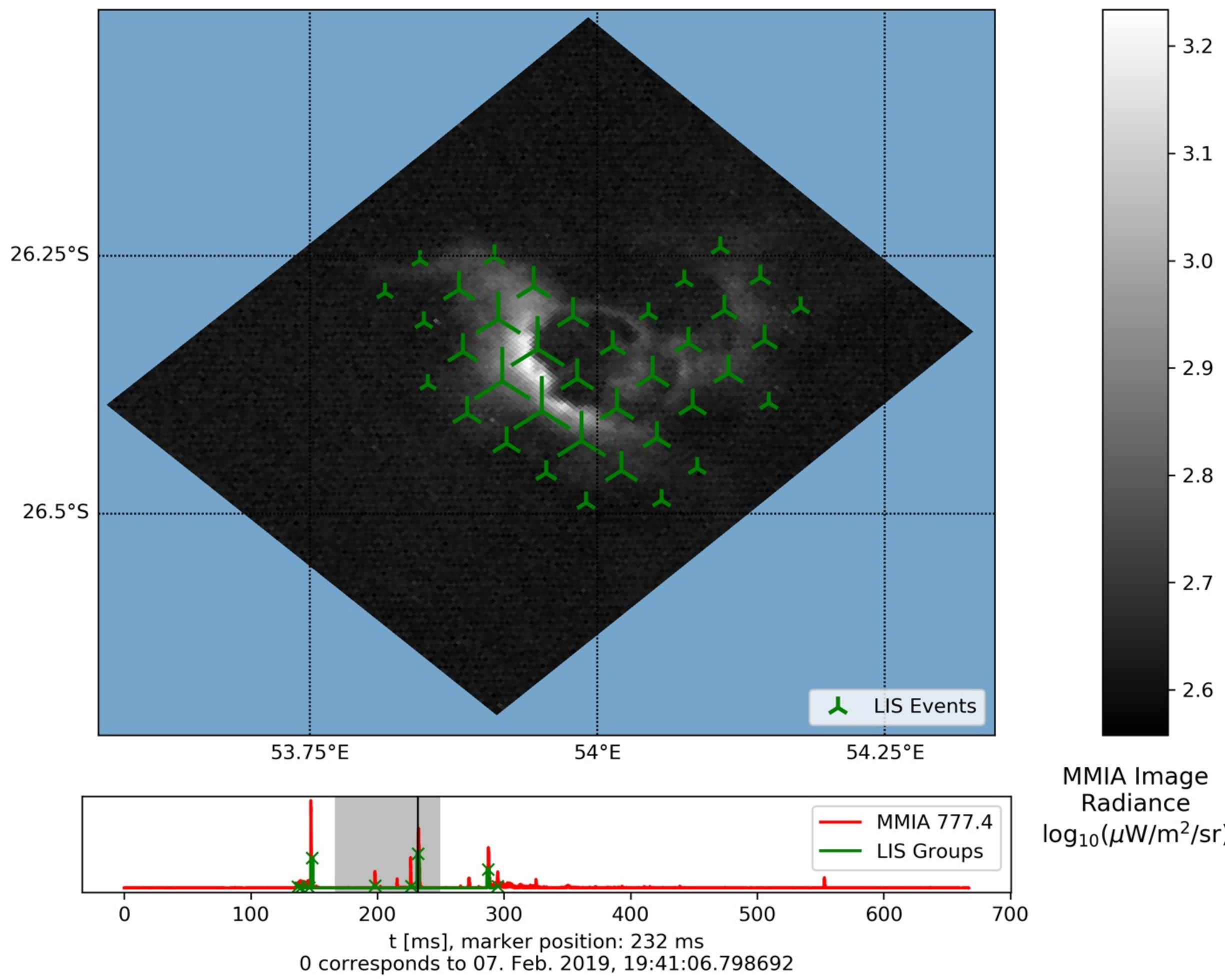

Figure 12. Comparison of ASIM and ISS LIS observations of a lightning flash over Madagascar. (top) an image of the lightning flash captured by the ASIM camera with ISS LIS events from the group closest in time to the frame (i.e., black line in bottom panel) plotted as green symbols whose size correspond to the radiance measured by the LIS camera and scaled (10^{-4}) to match the same units of ASIM radiance, which are given in logarithmic scale to enhance the illuminated pixels. (bottom) time-series of ASIM 777.4 nm photometer (red) and LIS groups (green) with the shaded region corresponding to the duration of the ASIM camera frame.

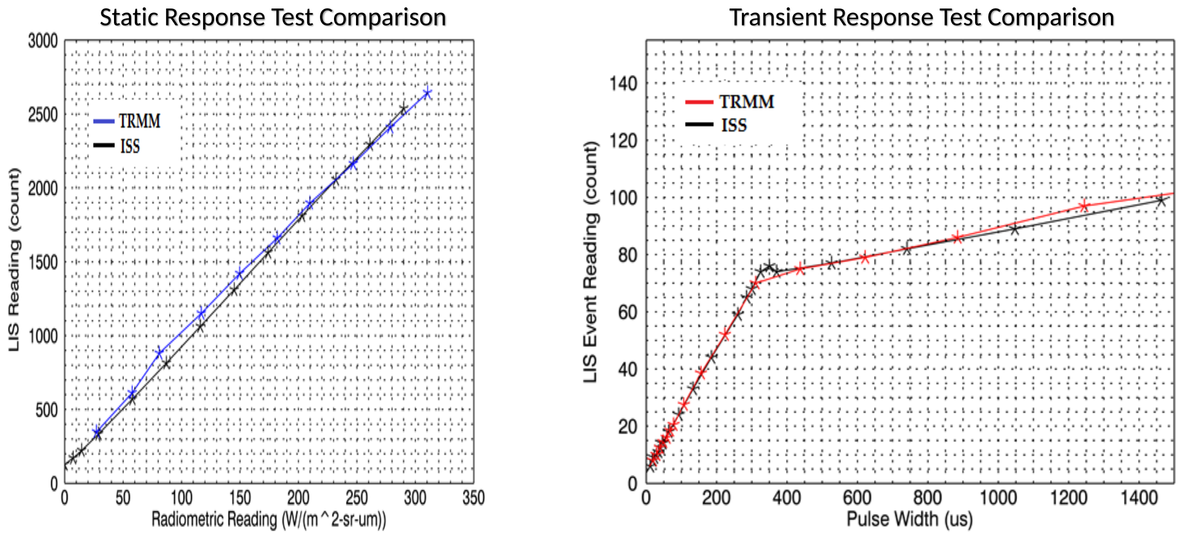

Figure A1. The close comparison between the original TRMM LIS calibration (OC; labeled TRMM) and the retest calibration (RC) of ISS LIS (labeled ISS). for a representative subset of the instrument's FOV. Left: Static Response Test. Right: Transient Response Test.